

Cytidine and ribothymidine nucleolipids synthesis, organogelation, selective anion and metal ion responsiveness

Ashok Nuthanakanti*

Department of Chemistry, Indian Institute of Science Education and Research (IISER) Pune
Dr. Homi Bhabha Road, Pashan, Pune 411008, India. E-mail: ashok199919@gmail.com.

Electronic Supplementary Information

| Content | Page |
|---|---------|
| 1. Materials | S2 |
| 2. Instrumentation | S2 |
| 3. Characterization data for compounds 4a–4b, 7a–7e and 8a–8b | S2-S6 |
| Fig. S1 Strain sweep rheological measurements of nucleolipid organogels | S7 |
| Fig. S2 Single-crystal X-ray structure of nucleolipids (A) 7a and (B) 7b | S7 |
| Table S1. H-bonding distances and angles, torsional angles | S8 |
| Fig. S3 (A) 1D-sheet formed by H-bonding interactions | S8 |
| Fig. S4 X-ray crystal structure of nucleolipid 7b showing a strong CH- π stacking interaction | S9 |
| Table S2. Crystallographic data for nucleolipid 7a | S9-S10 |
| Table S3. Crystallographic data for nucleolipid 7b | S10 |
| 4. Variable temperature ¹H NMR experiments | S11 |
| Fig. S5 Partial ¹ H NMR spectra of nucleolipid gels of 7b (3.2 w/v %) (A) and 7c (B) | S11-S12 |
| Fig. S6 ¹ H NMR spectra of nucleolipid gels of (A) 7b (3.2 w/v %) and (B) 7c (2.1 w/v %) | S13-S14 |
| 5. Powder X-ray diffraction (PXRD) analysis of nucleolipid | S14-S15 |
| Fig. S7 Comparison of PXRD spectra of xerogels of 7b obtained from (A) DMF | S15 |
| Fig. S8 Partial ¹ H NMR spectrum of nucleolipid 7b in <i>d</i> ₆ -DMSO (3.2 w/v %) | S16 |
| Fig. S9 ¹ H NMR spectrum of nucleolipid 7b in <i>d</i> ₆ -DMSO (3.2 w/v %) | S17 |
| Fig. S10 ¹ H NMR spectrum of nucleolipid 7b in <i>d</i> ₆ -DMSO (3.2 w/v %) | S18 |
| Fig. S11 FESEM image of nucleolipid 7d gel (A) in the absence and (B) in the presence of Hg ²⁺ ions. | S18 |
| Fig. S12 Mass spectrum showing the molecular ion peak of the 7d -Hg- 7d base pair complex | S19 |
| Fig. S13 (A) Mass spectrum showing the molecular ion peak of the 7b -Hg- 7b base pair complex | S19 |
| 6. NMR | S20-S28 |

1. Materials: tert-Butyl(chloro)dimethylsilane (TBDMS-Cl), ribothymidine, 4,4'-dimethoxytrityl chloride (DMT-Cl), dodecanoic acid, palmitic acid, stearic acid, oleic acid, tetrabutylammonium salts (fluoride, chloride, bromide, iodide, acetate, sulfate and azide), silver nitrate, zinc nitrate hexahydrate, lead(II) nitrate, cadmium acetate dihydrate, mercury(II) perchlorate hexahydrate, cytidine and dry pyridine were purchased from Sigma-Aldrich. EDC (1-(3-dimethyl aminopropyl)-3-ethyl carbodiimide hydrochloride) and 4-dimethylaminopyridine were obtained from Avra Synthesis. Myristic acid was procured from Fluka. Silicon wafers (N-type without dopant) were purchased from Sigma-Aldrich.

2. Instrumentation: NMR spectra were recorded on 400 MHz Jeol ECS-400 spectrometer and Bruker 500 MHz spectrometer. The morphology of gels was analyzed using Zeiss Ultra Plus field-emission scanning electron microscope (FESEM). Powder X-ray diffraction (PXRD) spectra were recorded at room temperature using Bruker D8 Advance diffractometer (Cu K α radiation, $\lambda = 1.5406 \text{ \AA}$). Single crystal X-ray data for structure determination were collected from Bruker APEX II DUO diffractometer using CuK α ($\lambda = 1.54178 \text{ \AA}$) and MoK α ($\lambda = 0.71073 \text{ \AA}$) graphite monochromated radiation. Rheology measurements were carried out in Anton paar MCR 302 instrument. Matrix-assisted laser desorption/ionization time-of-flight (MALDI-TOF) mass spectrometric analysis was used for a ribothymidine-Hg-ribothymidine dimer formation. Mass measurements were recorded on Applied Biosystems 4800 Plus MALDI TOF/TOF analyzer and Water Synapt G2 High Definition mass spectrometers.

3. Characterization data for compounds 4a–4b, 7a–7e and 8a–8b

Synthesis of 5'-O-TBDMS-cytidine (2): The reaction mixture of cytidine (1 g, 4.11 mM, and 1.0 equiv.) and anhydrous DMF (5 mL/g) was dissolved at RT. Then TBDMS-Cl (0.743 g, 4.93 mM, and 1.2 equiv.) and imidazole (0.58 g, 8.83 mM, and 2.1 equiv.) were added to cytidine suspension, and allowed to stir at RT for 12 h under nitrogen atmosphere. The resultant residue was diluted with dichloromethane and extracted with NaHCO₃ and dried over sodium sulfate. The residue was purified by silica gel column chromatography (7% methanol in dichloromethane) to afford the products (2).

2: Colourless solid, 74% yield. TLC (methanol:CH₂Cl₂ = 5:95); R_f = 0.35; ¹H NMR (400 MHz, CDCl₃): δ (ppm) 7.95 (d, $J = 7.6 \text{ Hz}$, 1H), 5.93 (d, $J = 2.0 \text{ Hz}$, 1H), 5.76 (d, $J = 7.2 \text{ Hz}$, 1H), 4.16 (br, 3H), 3.96–3.93 (m, 1H), 3.81–3.78 (m, 1H), 0.87 (s, 9H), 0.06 (s, 6H); ¹³C

NMR (100 MHz, CDCl₃): δ (ppm) 165.8, 157.3, 141.3, 94.9, 91.2, 85.6, 70.2, 62.7, 26.1, 18.5, -5.3, -5.4. HRMS: m/z Calcd. for C₁₅H₂₈N₃O₅Si [M+H]⁺ = 358.1798, found = 358.1803.

3a: Colourless solid, 26% yield. TLC (methanol:CH₂Cl₂= 5:95); R_f = 0.42; ¹H NMR (400 MHz, CDCl₃): δ (ppm) 7.91 (d, J = 7.6 Hz, 1H), 6.36 (d, J = 6.0 Hz, 1H), 5.69 (d, J = 7.6 Hz, 1H), 5.37–5.35 (m, 1H), 5.30–5.27 (m, 1H), 4.17–4.15 (m, 1H), 3.94 (dd, J_1 = 11.6 Hz, J_2 = 2.0 Hz, 1H), 3.81 (dd, J_1 = 11.6 Hz, J_2 = 1.6 Hz, 1H), 2.33–2.28 (m, 4H), 1.64–1.54 (m, 4 H), 1.25–1.24 (m, 32 H), 0.93 (s, 9H), 0.89–0.85 (m, 6 H), 0.13 (s, 3H), 0.12 (s, 3 H); ¹³C NMR (100 MHz, CDCl₃): δ (ppm) 172.8, 172.5, 165.6, 155.8, 141.4, 94.9, 86.5, 83.1, 74.1, 70.8, 62.8, 34.2, 34.0, 32.1, 29.8, 29.6, 29.5, 29.4, 29.4, 29.3, 29.3, 26.0, 25.0, 24.9, 22.8, 18.5, 14.2, -5.2, -5.4. HRMS: m/z Calcd. for C₃₉H₇₂N₃O₇Si [M+H]⁺ = 722.5139, found = 722.5132.

3b: Colourless solid, 28% yield. TLC (methanol:CH₂Cl₂= 5:95); R_f = 0.43; ¹H NMR (400 MHz, CDCl₃): δ (ppm) 7.81 (d, J = 7.2 Hz, 1H), 6.35 (d, J = 5.6 Hz, 1H), 5.70 (d, J = 7.6 Hz, 1H), 5.37–5.34 (m, 1H), 5.29–5.26 (m, 1H), 4.16–4.15 (m, 1H), 3.94 (dd, J_1 = 11.2 Hz, J_2 = 1.8 Hz, 1H), 3.80 (dd, J_1 = 11.6 Hz, J_2 = 1.6 Hz, 1H), 2.34–2.28 (m, 4H), 1.61–1.53 (m, 4 H), 1.27–1.24 (m, 40 H), 0.93 (s, 9H), 0.87–0.84 (m, 6 H), 0.12 (s, 3H), 0.11 (s, 3 H); ¹³C NMR (100 MHz, CDCl₃): δ (ppm) 172.8, 172.6, 165.6, 155.7, 141.3, 95.1, 86.5, 83.1, 74.1, 70.8, 62.8, 34.1, 34.0, 32.1, 29.8, 29.6, 29.6, 29.5, 29.4, 29.3, 29.2, 26.0, 24.9, 24.9, 22.8, 18.5, 14.3, -5.4, -5.5. HRMS: m/z Calcd. for C₄₃H₈₀N₃O₇Si [M+H]⁺ = 778.5765, found = 778.5767.

4a: Colourless solid, 71% yield over two steps. TLC (methanol:CH₂Cl₂= 5:95); R_f = 0.36; ¹H NMR (400 MHz, CDCl₃): δ (ppm) 7.63 (d, J = 7.2 Hz, 1H), 5.86–5.82 (m, 2H), 5.60 (t, J = 5.2 Hz, 1H), 5.51 (t, J = 5.0 Hz, 1H), 4.18–4.17 (m, 1H), 3.97–3.94 (m, 1H), 3.79–3.76 (m, 1H), 2.34–2.26 (m, 4H), 1.65–1.55 (m, 4 H), 1.25–1.24 (m, 32 H), 0.89–0.85 (m, 6 H); ¹³C NMR (100 MHz, CDCl₃): δ (ppm) 172.9, 172.6, 166.1, 156.2, 142.8, 96.0, 90.6, 83.6, 73.3, 70.8, 61.3, 34.2, 34.0, 32.0, 29.8, 29.6, 29.5, 29.4, 29.3, 29.3, 26.0, 25.0, 24.9, 22.8, 14.2. HRMS: m/z Calcd. for C₃₃H₅₈N₃O₇ [M+H]⁺ = 608.4275, found = 608.4276.

4b: Colourless solid, 77% yield over two steps. TLC (methanol:CH₂Cl₂= 5:95); R_f = 0.31; ¹H NMR (400 MHz, CDCl₃): δ (ppm) 7.64 (d, J = 7.2 Hz, 1H), 5.84–5.82 (m, 2H), 5.59 (t, J = 5.2 Hz, 1H), 5.51 (t, J = 5.2 Hz, 1H), 4.18–4.17 (m, 1H), 3.98–3.95 (m, 1H), 3.79–3.76 (m, 1H), 2.35–2.27 (m, 4H), 1.65–1.54 (m, 4 H), 1.29–1.25 (m, 40 H), 0.89–0.86 (m, 6 H); ¹³C NMR (100 MHz, CDCl₃): δ (ppm) 173.0, 172.6, 166.0, 156.1, 143.0, 95.8, 91.1, 83.4, 73.4,

70.5, 61.4, 34.2, 34.1, 32.1, 29.9, 29.8, 29.7, 29.5, 29.5, 29.3, 29.3, 25.0, 25.0, 22.8, 14.2.
HRMS: m/z Calcd. for C₃₇H₆₆N₃O₇ [M+H]⁺ = 664.4901, found = 664.4877.

Synthesis of 5'-dimethyltritoxyribothymidine (6): Dimethoxytritylchloride (2.97 g, 8.76 mM, 1.3 equiv.), ribothymidine (1.74 g, 6.74 mM, 1.0 equiv.) and a catalytic amount of N,N-dimethyl aminopyridine (0.08 g, 0.66 mM, 0.1 equiv.) were dissolved in 20 mL of dry pyridine. The reaction mixture was stirred for 12 hours at room temperature under nitrogen atmosphere. Pyridine was removed under vacuum and the resulting crude material was washed with 5% NaHCO₃, the product was extracted with methylene chloride. The organic phase was dried over sodium sulfate and purified on silica gel column chromatography (2.5 % methanol in CH₂Cl₂ containing 1% triethylamine) to afford the product as white foam (3.4 g, 75 % yield).

6: Colourless solid, 75% yield. TLC (CH₂Cl₂:MeOH = 95:5 with few drops of Et₃N); R_f = 0.53; ¹H NMR (400 MHz, CDCl₃): δ (ppm) 7.69 (d, *J* = 1.2 Hz, 1H), 7.40–7.38 (m, 2H), 7.30–7.27 (m, 5H), 7.22–7.18 (m, 1H), 6.84–6.80 (m, 4H), 5.96 (d, *J* = 3.2 Hz, 1H), 4.43–4.39 (m, 2H), 4.20–4.19 (m, 1H), 3.77 (s, 3H), 3.76 (s, 3H), 3.50 (dd, *J*₁ = 10.8 Hz, *J*₂ = 2.4 Hz, 1H), 3.38 (dd, *J*₁ = 10.8 Hz, *J*₂ = 2.8 Hz, 1H), 1.39 (d, *J* = 1.2 Hz, 3H); ¹³C NMR (100 MHz, CDCl₃): δ (ppm) 164.6, 158.8, 158.8, 151.5, 144.5, 136.0, 135.5, 135.4, 130.2, 128.2, 128.1, 127.2, 113.4, 111.3, 89.9, 87.0, 84.2, 75.4, 70.6, 62.8, 55.4, 10.5; HRMS: m/z Calcd. for C₃₁H₃₂N₂O₈Na [M+Na]⁺ = 583.2056, found = 583.2050.

7a: Colourless solid, 70% yield over two steps. TLC (EtOAc:hexane = 30:70); R_f = 0.42; ¹H NMR (400 MHz, CDCl₃): δ (ppm) 8.68 (br, 1H), 7.46 (d, *J* = 0.8 Hz, 1H), 6.02–5.98 (m, 1H), 5.49–5.46 (m, 2H), 4.18–4.17 (m, 1H), 3.95 (dd, *J*₁ = 12.2 Hz, *J*₂ = 2.2 Hz, 2H), 3.86 (dd, *J*₁ = 12.0 Hz, *J*₂ = 2.4 Hz, 1H), 2.36–2.29 (m, 4H), 1.92 (d, *J* = 1.2 Hz, 3H), 1.66–1.54 (m, 4H), 1.29–1.25 (m, 32H), 0.89–0.85 (m, 6H); ¹³C NMR (100 MHz, CDCl₃): δ (ppm) 173.0, 172.7, 163.6, 150.6, 136.6, 111.8, 88.1, 83.6, 72.7, 71.0, 62.1, 34.2, 33.9, 32.1, 29.8, 29.6, 29.5, 29.4, 29.4, 29.3, 29.2, 25.0, 24.9, 22.8, 14.3, 12.7; HRMS: m/z Calcd. for C₃₄H₅₈N₂O₈Na [M+Na]⁺ = 645.4090, found = 645.4095.

7b: Colourless solid, 68% yield over two steps. TLC (EtOAc:hexane = 40:60); R_f = 0.48; ¹H NMR (400 MHz, CDCl₃): δ (ppm) 8.58–8.47 (br, 1H), 7.45 (s, 1H), 6.01–5.98 (m, 1H), 5.50–5.46 (m, 2H), 4.18–4.17 (m, 1H), 3.95 (dd, *J*₁ = 12.2 Hz, *J*₂ = 2.2 Hz, 1H), 3.86 (dd, *J*₁ = 12.2 Hz, *J*₂ = 2.2 Hz, 1H), 2.38–2.29 (m, 4H), 1.92 (d, *J* = 0.8 Hz, 3H), 1.66–1.54 (m, 4H),

1.29–1.24 (m, 40H), 0.89–0.86 (m, 6H); ^{13}C NMR (100 MHz, CDCl_3): δ (ppm) 173.0, 172.7, 163.5, 150.5, 136.5, 111.8, 88.1, 83.6, 72.7, 71.0, 62.1, 34.2, 34.0, 32.1, 29.8, 29.8, 29.6, 29.5, 29.4, 29.4, 29.3, 29.2, 25.0, 24.9, 25.0, 24.9, 22.8, 14.3, 12.7; HRMS: m/z Calcd. for $\text{C}_{38}\text{H}_{66}\text{N}_2\text{O}_8\text{Na}$ $[\text{M}+\text{Na}]^+ = 701.4716$, found = 701.4711.

7c: Colourless solid, 62% yield over two steps. TLC (EtOAc:hexane = 40:60); $R_f = 0.43$; ^1H NMR (400 MHz, CDCl_3): δ (ppm) 8.54 (br, 1H), 7.46 (br, 1H), 6.01–5.98 (m, 1H), 5.50–5.46 (m, 2H), 4.18–4.17 (m, 1H), 3.95 (dd, $J_1 = 12.2$ Hz, $J_2 = 1.8$ Hz, 1H), 3.86 (dd, $J_1 = 12.2$ Hz, $J_2 = 2.4$ Hz, 1H), 2.38–2.29 (m, 4H), 1.92 (d, $J = 0.8$ Hz, 3H), 1.66–1.54 (m, 4H), 1.29–1.25 (m, 48H), 0.89–0.86 (m, 6H); ^{13}C NMR (100 MHz, CDCl_3): δ (ppm) 173.0, 172.7, 163.5, 150.5, 136.5, 111.8, 88.1, 83.6, 72.7, 71.0, 62.1, 34.2, 34.0, 32.1, 29.9, 29.8, 29.6, 29.5, 29.4, 29.3, 29.2, 25.0, 24.9, 22.8, 14.3, 12.7; HRMS: m/z Calcd. for $\text{C}_{42}\text{H}_{74}\text{N}_2\text{O}_8\text{Na}$ $[\text{M}+\text{Na}]^+ = 757.5342$, found = 757.5341.

7d: Colourless solid, 85% yield over two steps. TLC (EtOAc:hexane = 40:60); $R_f = 0.48$; ^1H NMR (400 MHz, CDCl_3): δ (ppm) 8.60–8.49 (br, 1H), 7.46 (s, 1H), 6.01–5.98 (m, 1H), 5.49–5.46 (m, 2H), 4.18–4.17 (m, 1H), 3.95 (dd, $J_1 = 12.0$ Hz, $J_2 = 2.0$ Hz, 1H), 3.86 (dd, $J_1 = 12.2$ Hz, $J_2 = 2.0$ Hz, 1H), 2.37–2.29 (m, 4H), 1.92 (s, 3H), 1.64–1.54 (m, 4H), 1.29–1.26 (m, 56H), 0.89–0.86 (m, 6H); ^{13}C NMR (100 MHz, CDCl_3): δ (ppm) 173.0, 172.7, 163.5, 150.5, 136.5, 111.8, 88.1, 83.6, 72.7, 71.0, 62.1, 34.2, 34.0, 32.1, 29.9, 29.7, 29.5, 29.5, 29.3, 29.2, 25.0, 24.9, 22.8, 14.3, 12.7; HRMS: m/z Calcd. for $\text{C}_{46}\text{H}_{82}\text{N}_2\text{O}_8\text{Na}$ $[\text{M}+\text{Na}]^+ = 813.5968$, found = 813.5966.

7e: Colourless solid, 64% yield over two steps. TLC (EtOAc:hexane = 40:60); $R_f = 0.42$; ^1H NMR (400 MHz, CDCl_3): δ (ppm) 8.76 (br, 1H), 7.47 (s, 1H), 6.02–5.99 (m, 1H), 5.49–5.45 (m, 2H), 5.38–5.30 (m, 4H), 4.18–4.17 (m, 1H), 3.95 (dd, $J_1 = 12.0$ Hz, $J_2 = 2.0$ Hz, 1H), 3.86 (dd, $J_1 = 12.0$ Hz, $J_2 = 2.4$ Hz, 1H), 2.36–2.29 (m, 4H), 2.07–1.98 (m, 8H), 1.92 (d, $J = 0.8$ Hz, 3H), 1.64–1.54 (m, 4H), 1.30–1.25 (m, 40H), 0.89–0.85 (m, 6H); ^{13}C NMR (100 MHz, CDCl_3): δ (ppm) 173.0, 172.7, 163.7, 150.6, 136.6, 130.4, 130.2, 129.9, 129.8, 128.2, 128.0, 111.8, 88.0, 83.6, 72.8, 71.0, 62.1, 34.1, 33.9, 32.1, 29.9, 29.9, 29.8, 29.7, 29.5, 29.3, 29.3, 29.2, 27.4, 27.3, 25.0, 24.8, 22.8, 14.3, 12.7; HRMS: m/z Calcd. for $\text{C}_{46}\text{H}_{79}\text{N}_2\text{O}_8$ $[\text{M}+\text{H}]^+ = 787.5836$, found = 787.5813.

General procedure for synthesis of trifatty acid-substituted nucleolipids 8a–8b.
ribothymidine (1.0 equiv.), fatty acid (myristic acid and palmitic acid, 3.2 equiv.), EDC (3.2

equiv.), and DMAP (0.35 equiv.) were dissolved in anhydrous dichloromethane. The reaction mixture was stirred for 12 h at RT under nitrogen atmosphere. The reaction mixture was diluted with dichloromethane and extracted with saturated NH_4Cl solution. The organic extract was dried over sodium sulfate and filtered, and the filtrate was evaporated. The residue was purified by silica gel column chromatography (40% ethyl acetate in hexane) to afford the products.

8a: Colourless solid, 93% yield. TLC (EtOAc:hexane = 40:60); R_f = 0.65; ^1H NMR (400 MHz, CDCl_3): δ (ppm) 8.59 (br, 1H), 7.19 (br, 1H), 6.09 (d, J = 5.2 Hz, 1H), 5.33–5.28 (m, 2H), 4.39 (dd, J_1 = 12.8 Hz, J_2 = 4.4 Hz, 1H), 4.33–4.30 (m, 2H), 2.42–2.29 (m, 6H), 1.94 (d, J = 0.8 Hz, 3H), 1.66–1.56 (m, 6H), 1.29–1.25 (m, 60H), 0.89–0.86 (m, 9H); ^{13}C NMR (100 MHz, CDCl_3): δ (ppm) 173.1, 172.7, 172.6, 163.4, 150.3, 135.0, 112.0, 86.8, 80.2, 72.5, 70.3, 63.3, 34.3, 34.0, 33.9, 32.1, 29.8, 29.7, 29.6, 29.6, 29.5, 29.4, 29.3, 29.2, 24.9, 24.8, 22.8, 14.3, 12.8; HRMS: m/z Calcd. for $\text{C}_{52}\text{H}_{93}\text{N}_2\text{O}_9$ $[\text{M}+\text{H}]^+$ = 889.6881, found = 889.6874.

8b: Colourless solid, 90% yield. TLC (EtOAc:hexane = 40:60); R_f = 0.62; ^1H NMR (400 MHz, CDCl_3): δ (ppm) 8.47 (br, 1H), 7.19 (d, J = 1.6 Hz, 1H), 6.09 (d, J = 5.2 Hz, 1H), 5.33–5.28 (m, 2H), 4.39 (dd, J_1 = 12.8 Hz, J_2 = 4.4 Hz, 1H), 4.33–4.30 (m, 2H), 2.40–2.29 (m, 6H), 1.94 (d, J = 0.8 Hz, 3H), 1.64–1.53 (m, 6H), 1.29–1.25 (m, 72H), 0.89–0.86 (m, 9H); ^{13}C NMR (100 MHz, CDCl_3): δ (ppm) 173.1, 172.6, 172.6, 163.3, 150.2, 135.0, 112.0, 86.8, 80.2, 72.5, 70.3, 63.3, 34.3, 34.0, 33.9, 32.1, 29.9, 29.8, 29.8, 29.6, 29.6, 29.5, 29.4, 29.3, 29.2, 25.0, 24.8, 22.8, 14.3, 12.8; HRMS: m/z Calcd. for $\text{C}_{58}\text{H}_{105}\text{N}_2\text{O}_9$ $[\text{M}+\text{H}]^+$ = 973.7820, found = 973.7808.

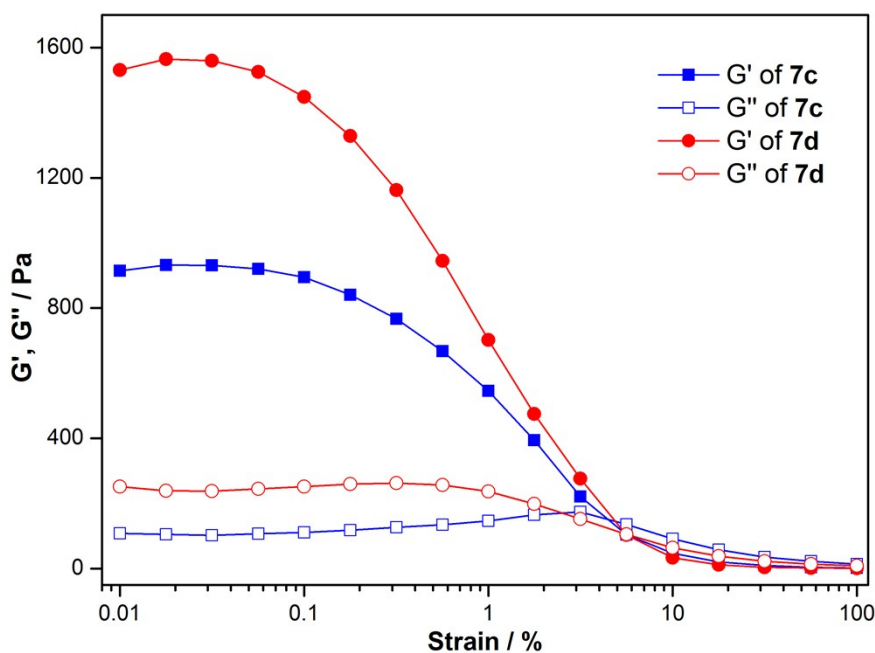


Fig. S1 Strain sweep rheological measurements of nucleolipid organogels of (A) **7c** (2.0 w/v %) and (B) **7d** (1.3 w/v %) were taken at respective CGC in DMSO at constant oscillating frequency.

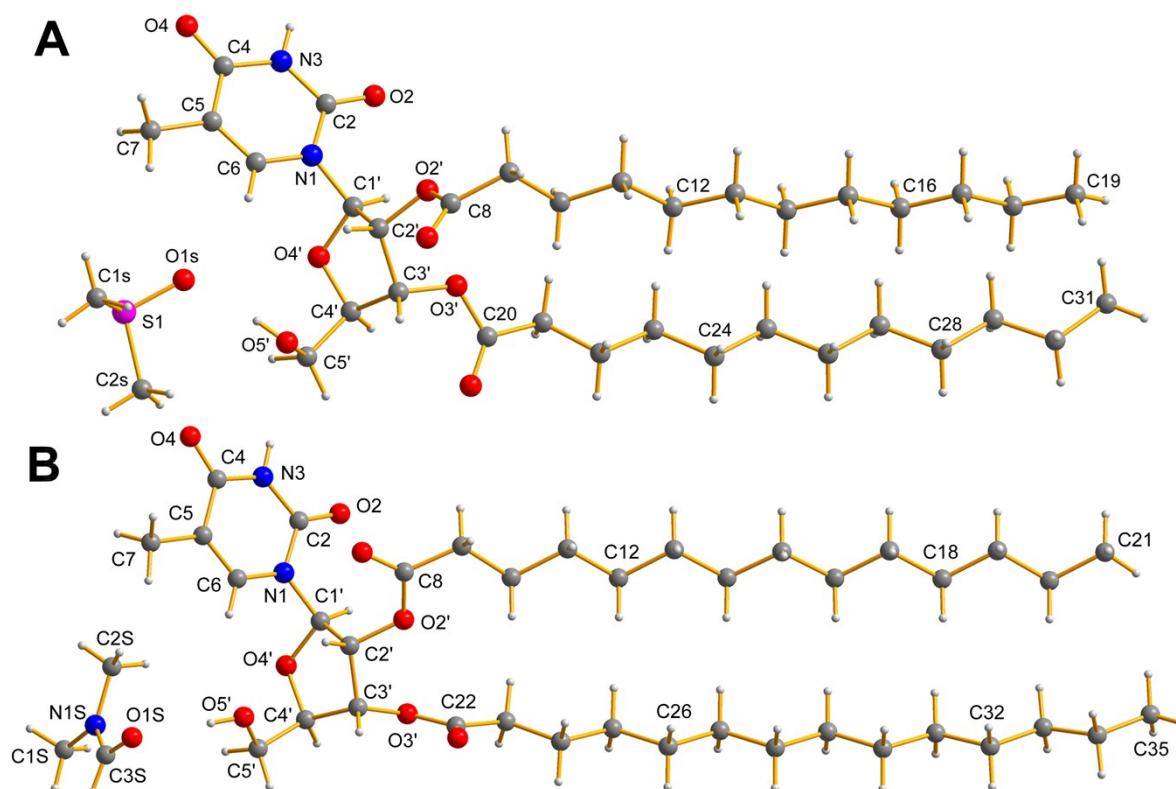


Fig. S2 Single-crystal X-ray structure of nucleolipids (A) **7a** and (B) **7b** showing one molecule in the unit cell and solvent molecule DMSO or DMF, respectively. Ribothymidine in all the nucleolipids adopts a C2'-endo *anti* conformation. Atoms are coded as follows: off white, hydrogen; dark gray, carbon; blue, nitrogen; red, oxygen; magenta, sulfur.

Table S1. H-bonding distances and angles, torsional angles measured from the crystal structure of ribothymidine nucleolipids **7a** and **7b**.

| Nucleolipid | Hydrogen bond | Distance (Å) | Angle (°) | Torsion angle (χ) (°) |
|-------------|---------------|--------------|-----------|------------------------------|
| 7a | N3H---O4 | 2.026(2) | 162.7(2) | C2-N1-C1'-O4' -124.7(3) |
| | O4---HN3 | 2.026(2) | 162.7(2) | |
| | C6H---O1s | 2.335(3) | 144.3(2) | |
| | O5'H---O1s | 1.912(3) | 169.1(2) | |
| 7b | N3H---O4 | 2.016(4) | 166.0(3) | C2-N1-C1'-O4' -127.8(5) |
| | O4---HN3 | 2.016(4) | 166.0(3) | |
| | C6H---O5' | 2.489(4) | 156.7(3) | |
| | O5'H---O1s | 1.895(4) | 168.3(3) | |

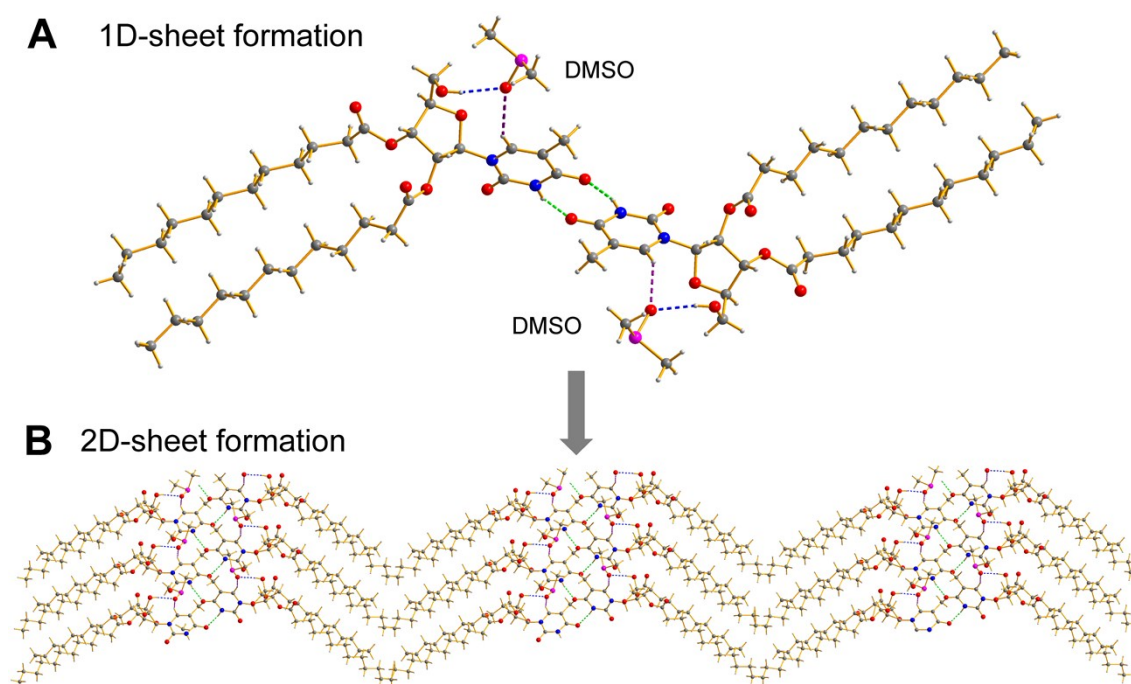


Fig. S3 (A) 1D-sheet formed by H-bonding interactions between the nucleobase and sugar-DMSO along the crystallographic b-axis (**7a**). (B) 2D-sheet formation by utilizing hydrophobic interactions of the acyl-chains non-interdigitation manner along the b-axes. Head to head and tail to tail interaction is clearly seen. Atoms are coded as follows: off white, hydrogen; dark gray, carbon; blue, nitrogen; red, oxygen; magenta, sulfur.

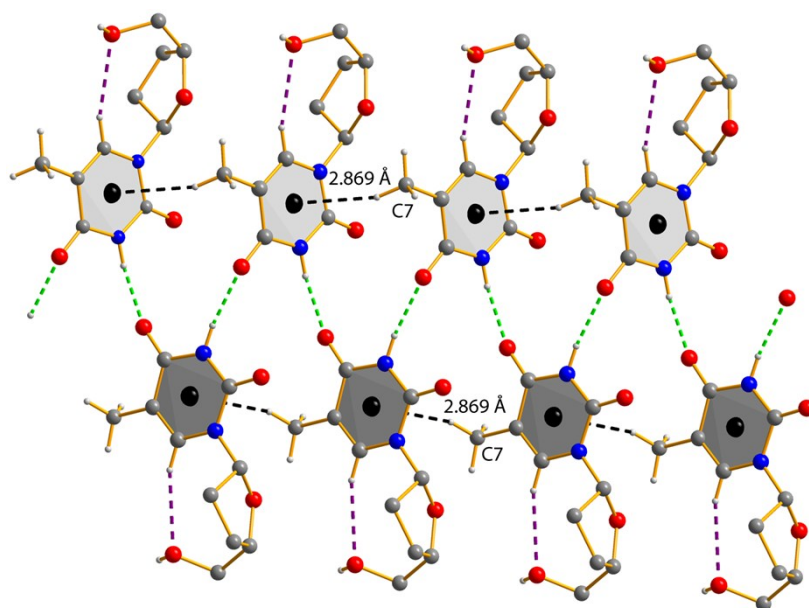


Fig. S4 X-ray crystal structure of nucleolipid **7b** showing a CH- π stacking interaction between the thymine methyl with adjacent thymine moiety along the crystallographic *a*-axes. The CH- π stacking distance (2.869 Å) between the methyl and thymine rings is shown in black dashed lines. A 1D hydrogen bonding interactions are shown in green and violet dashed lines. Other than H-bonding involving protons and long chain acyl chains are not shown for sake of clarity. Atoms are coded as follows: off white, hydrogen; dark gray, carbon; blue, nitrogen; red, oxygen.

Table S2. Crystallographic data for nucleolipid 7a

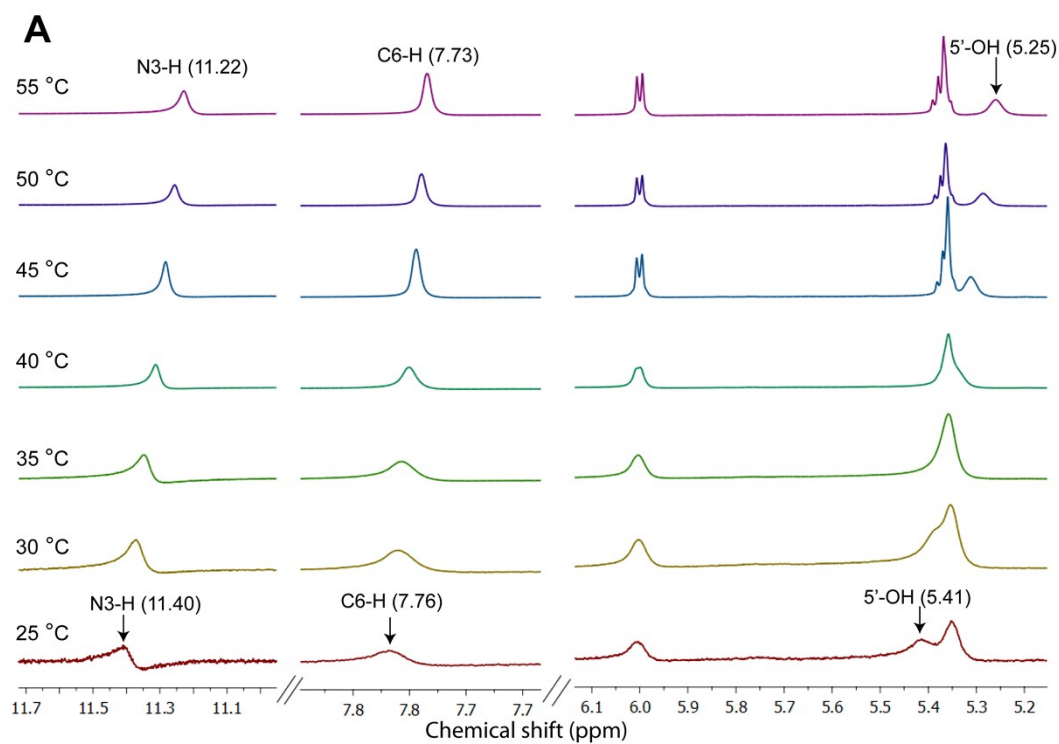
| | | |
|----------------------------------|---|---------------------|
| Compound identity | 7a | |
| Empirical formula | C ₃₆ H ₆₄ N ₂ O ₉ S | |
| Formula weight | 700.95 | |
| Temperature | 100(2) K | |
| Wavelength | 0.71073 Å | |
| Crystal system | Monoclinic | |
| Space group | C2 | |
| Unit cell dimensions | a = 17.373(3) | $\alpha = 90$ |
| | b = 5.5303(11) | $\beta = 95.254(4)$ |
| | c = 40.002(8) | $\gamma = 90$ |
| Volume | 3827.2(13) Å ³ | |
| Z | 4 | |
| Density (calculated) | 1.216 Mg/cm ³ | |
| Absorption coefficient (μ) | 0.138 mm ⁻¹ | |
| F(000) | 1528 | |
| Crystal size | 0.90 X 0.45 X 0.20 mm ³ | |
| Theta range for data collection | 2.36 to 28.27 | |
| Index ranges | -23 ≤ h ≤ 22, -7 ≤ k ≤ 7, -53 ≤ l ≤ 53 | |
| Reflections collected | 33021 | |
| Independent reflections | 9095 [R(int) = 0.0661] | |
| Completeness to theta = 72.85 | 99.9 % | |
| Absorption correction | MULTI-SCAN | |

| | |
|-----------------------------------|---|
| Max. and min. Transmission | 0.746 and 0.429 |
| Refinement method | Full-matrix least-squares on F ² |
| Data / restraints / parameters | 9095/ 1 / 439 |
| Goodness-of-fit on F ² | 1.043 |
| Final R indices [I>2sigma(I)] | R1 = 0.0599, wR2 = 0.1545 |
| R indices (all data) | R1 = 0.0718, wR2 = 0.1625 |
| Largest diff. Peak and hole | 0.416 and -0.526 e.Å ⁻³ |
| CCDC | 1829540 |

Table S3. Crystallographic data for nucleolipid 7b

| | |
|-----------------------------------|--|
| Compound identity | 7b |
| Empirical formula | C ₄₁ H ₇₃ N ₃ O ₉ |
| Formula weight | 752.02 |
| Temperature | 296(2) K |
| Wavelength | 1.54178 Å |
| Crystal system | Monoclinic |
| Space group | C2 |
| Unit cell dimensions | a = 21.4881(14) α = 90 b = 5.3392(3) β = 102.648(3) c = 38.114(2) γ = 90 |
| Volume | 4266.7(5) Å ³ |
| Z | 4 |
| Density (calculated) | 1.171 Mg/cm ³ |
| Absorption coefficient (μ) | 0.655 mm ⁻¹ |
| F(000) | 1648 |
| Crystal size | 0.36 X 0.17 X 0.06 mm ³ |
| Theta range for data collection | 2.37 to 72.85 |
| Index ranges | -26<=h<=26, -6<=k<=6, -47<=l<=47 |
| Reflections collected | 18271 |
| Independent reflections | 8551 [R(int) = 0.0424] |
| Completeness to theta = 72.85 | 98.9 % |
| Absorption correction | MULTI-SCAN |
| Max. and min. Transmission | 0.961 and 0.875 |
| Refinement method | Full-matrix least-squares on F ² |
| Data / restraints / parameters | 7217/ 1 / 484 |
| Goodness-of-fit on F ² | 1.648 |
| Final R indices [I>2sigma(I)] | R1 = 0.0886, wR2 = 0.2435 |
| R indices (all data) | R1 = 0.1044, wR2 = 0.2516 |
| Largest diff. Peak and hole | 0.473 and -0.354 e.Å ⁻³ |
| CCDC | 1829541 |

4. Variable temperature ^1H NMR experiments: Gels of **7b** (3.2 w/v %) and **7c** (2.1 w/v %) in d_6 -DMSO were formed in individual NMR tubes by heating and cooling process. ^1H NMR was recorded on a 500 MHz spectrometer as a function of increasing temperature. The temperature of the sample was elevated from 25 °C to 55 °C with an increment of 5 °C and equilibration time of 10 min. The spectrum was recorded at every 5 °C interval.



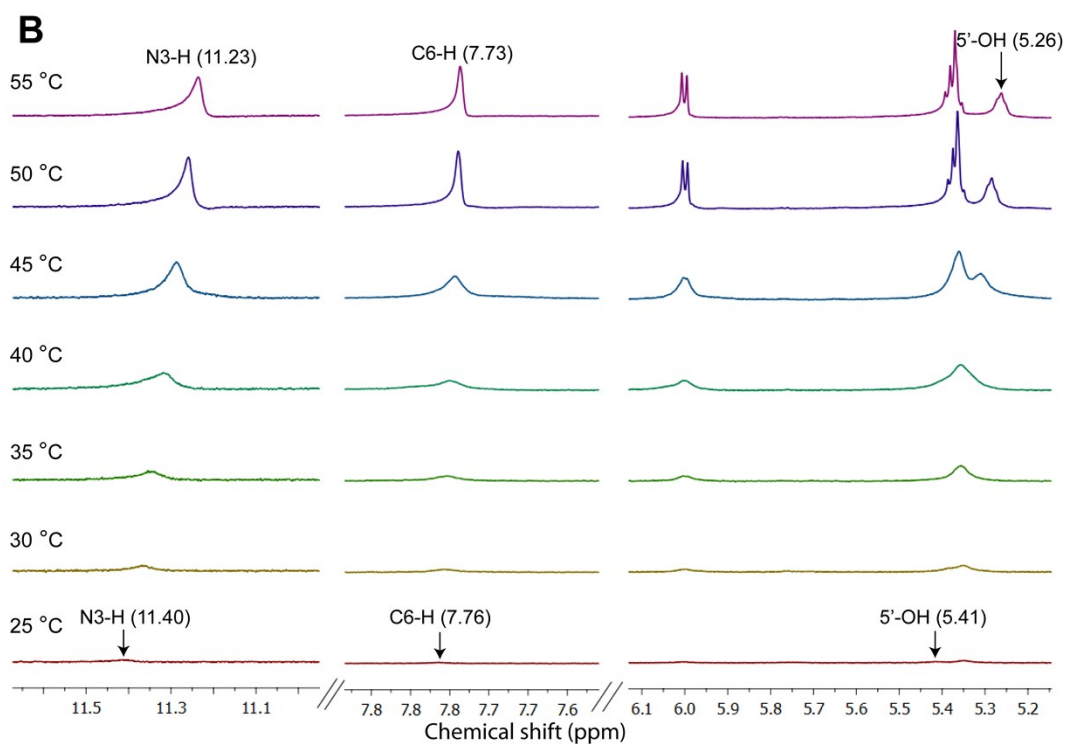
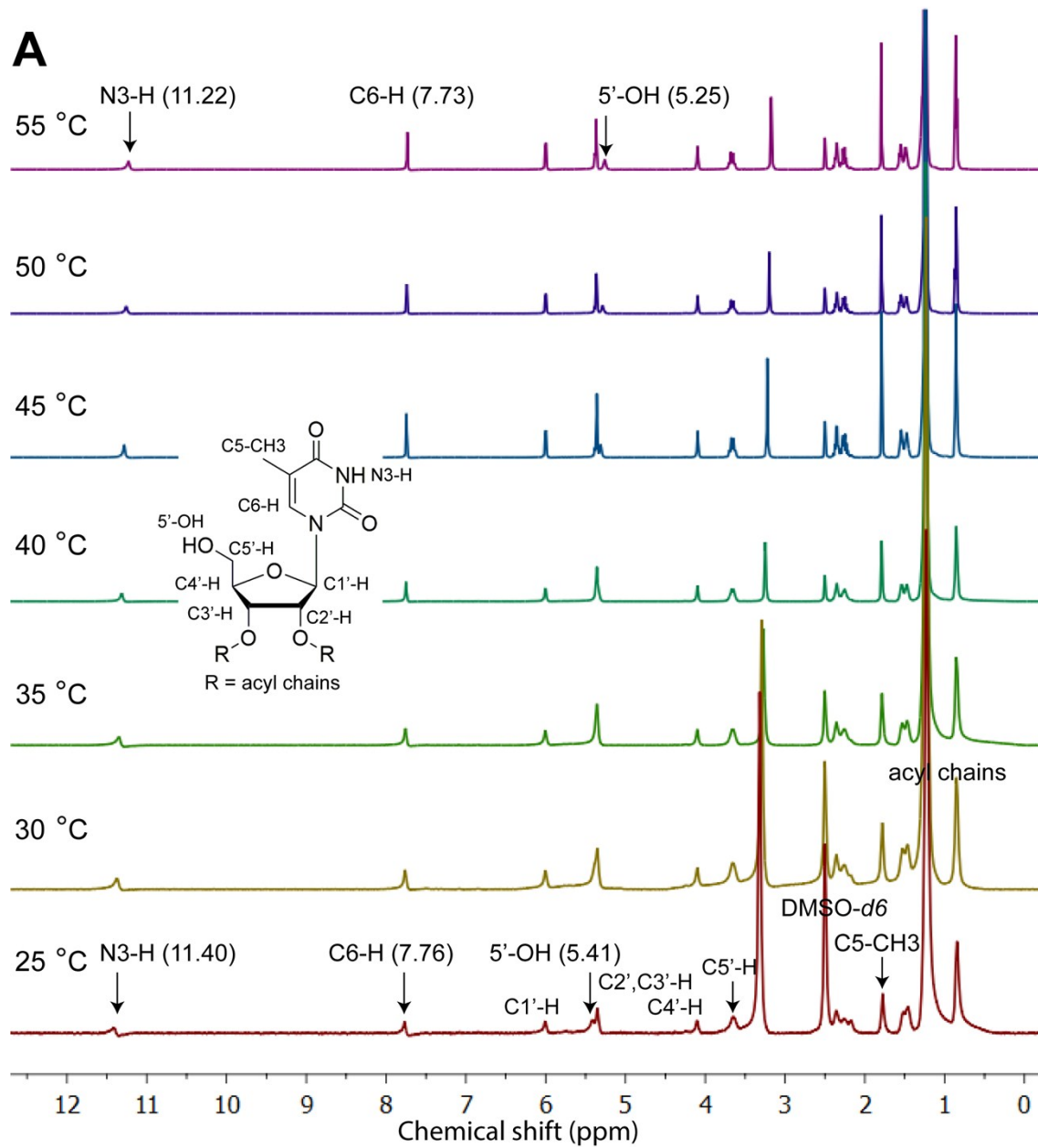


Fig. S5 Partial ^1H NMR spectra of nucleolipid gels of (A) **7b** (3.2 w/v %) and (B) **7c** (2.1 w/v %) in d_6 -DMSO as a function of increasing temperature. The N3-H, C6-H and 5'-OH protons are involved in strong intermolecular H-bonding in crystalline state, shown discernible up field shift in their proton signals during gel-sol transition. These results reveal that the H-bonding interactions in crystal structure and in gels are similar.



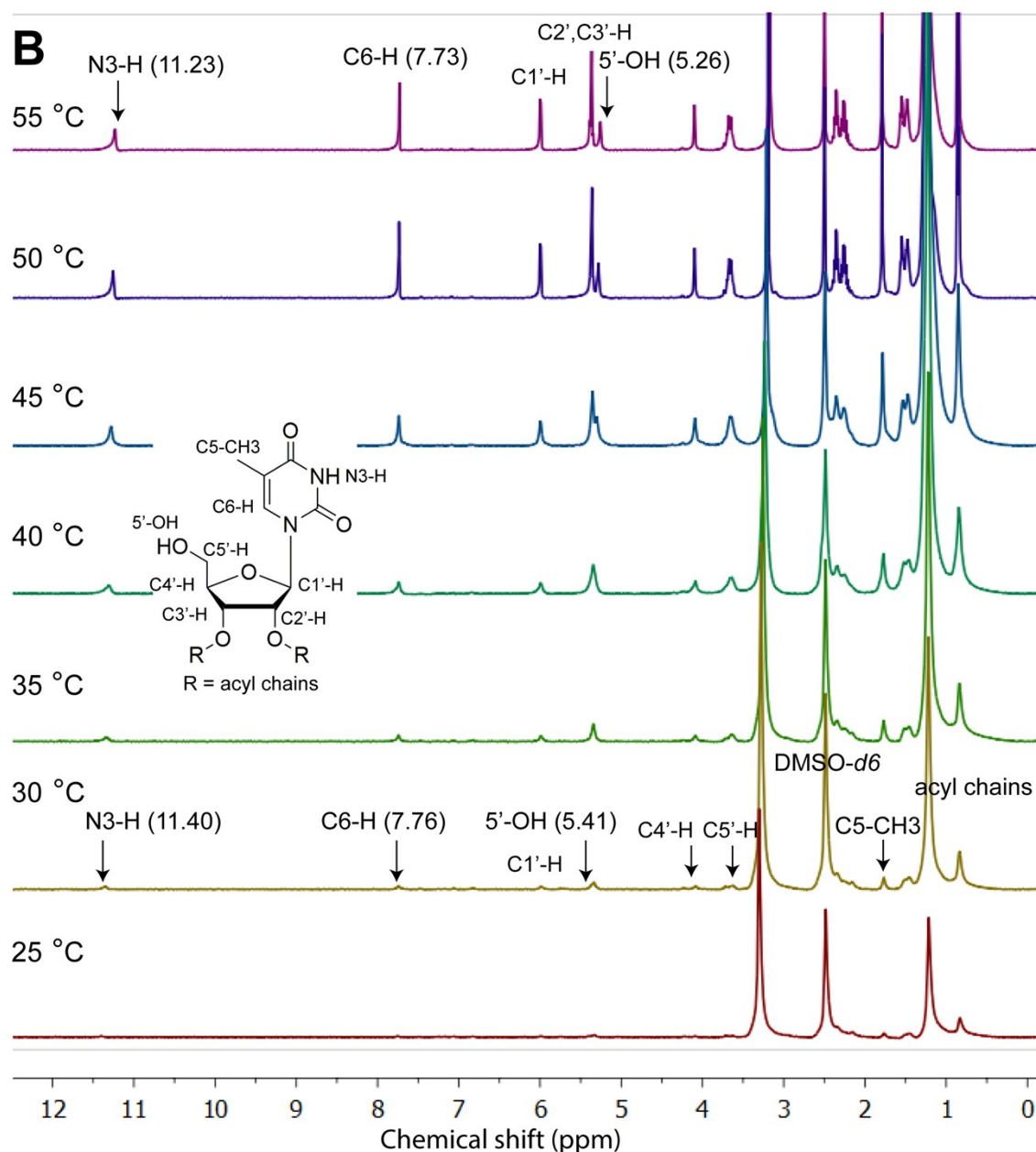


Fig. S6 ^1H NMR spectra of nucleolipid gels of (A) **7b** (3.2 w/v %) and (B) **7c** (2.1 w/v %) in d_6 -DMSO as a function of increasing temperature. The N3-H, C6-H and 5'-OH protons are involved in strong intermolecular H-bonding interactions, shown discernible up field shift in their proton signals during gel-sol transition.

5. Powder X-ray diffraction (PXRD) analysis of nucleolipid: Xerogels of **7b–7c** were formed by drop-casting a dispersion of the nucleolipid in different organic solvent (DMF) at its respective CGC. The samples were allowed to come to RT and were placed in a vacuum desiccator and dried under vacuum for nearly 12 h to obtain the xerogels. PXRD data was collected using Bruker D8 Advance diffractometer with $\text{CuK}\alpha$ source (1.5406 Å). Diffraction data were collected at 2θ angle from 1° to 25° using a 0.01° step size and 0.5 s per step. Low angle diffraction data was collected by keeping the motorized divergence slit in automatic

mode so as to maintain the X-ray beam footprint on the sample to 12 x 12 mm. Further, the position sensitive detector (Lynxeye) channels were reduced to minimize the background X-ray scattering entering the detector.

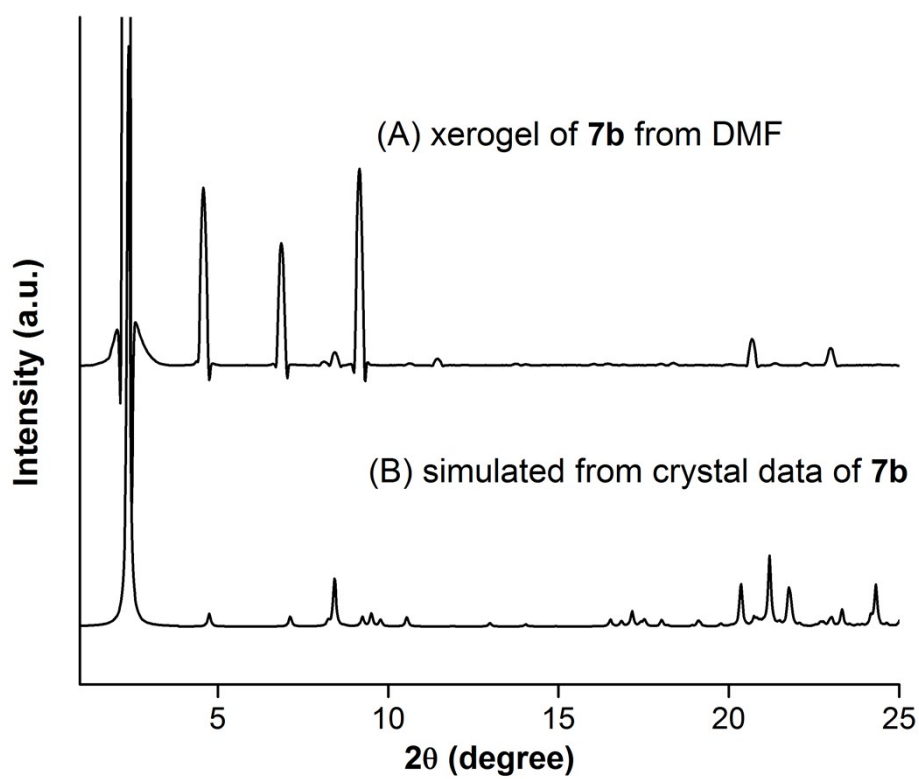


Fig. S7 Comparison of PXRD spectra of xerogels of **7b** obtained from (A) DMF and (B) PXRD pattern simulated from X-ray crystal data of **7b**.

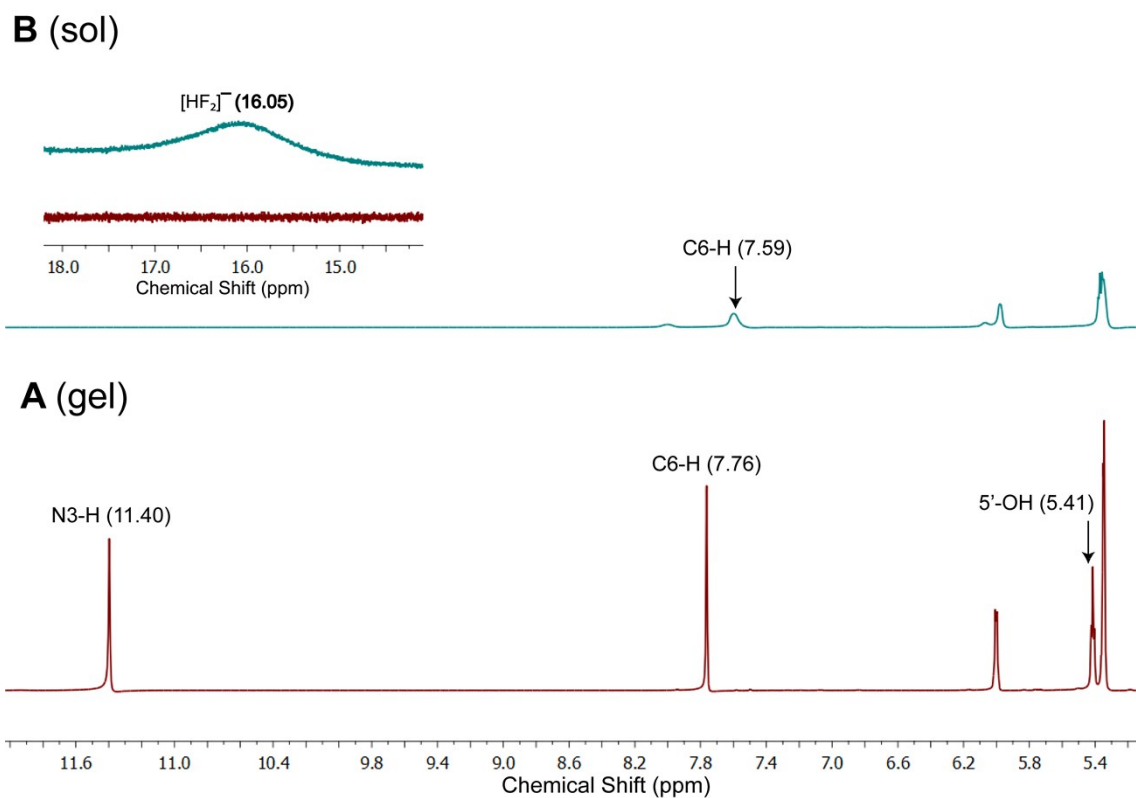


Fig. S8 Partial ^1H NMR spectrum of nucleolipid **7b** in d_6 -DMSO (3.2 w/v %) in the absence (**A**, gel state) and presence of 1 equiv. of fluoride ion (**B**, sol state). The disappearance of N3-H (11.40 ppm), 5'-OH (5.41 ppm) signals and appearance of a new triplet signal at 16.05 ppm corresponding to HF_2^- confirms the deprotonation of imino hydrogen atoms by fluoride anion. Similarly the C6-H (7.76 ppm) signal shifted towards up field C6-H (7.59 ppm) when the fluoride ion deprotonate N3-H. ^1H NMR spectra was obtained using Bruker 500 MHz spectrometer.

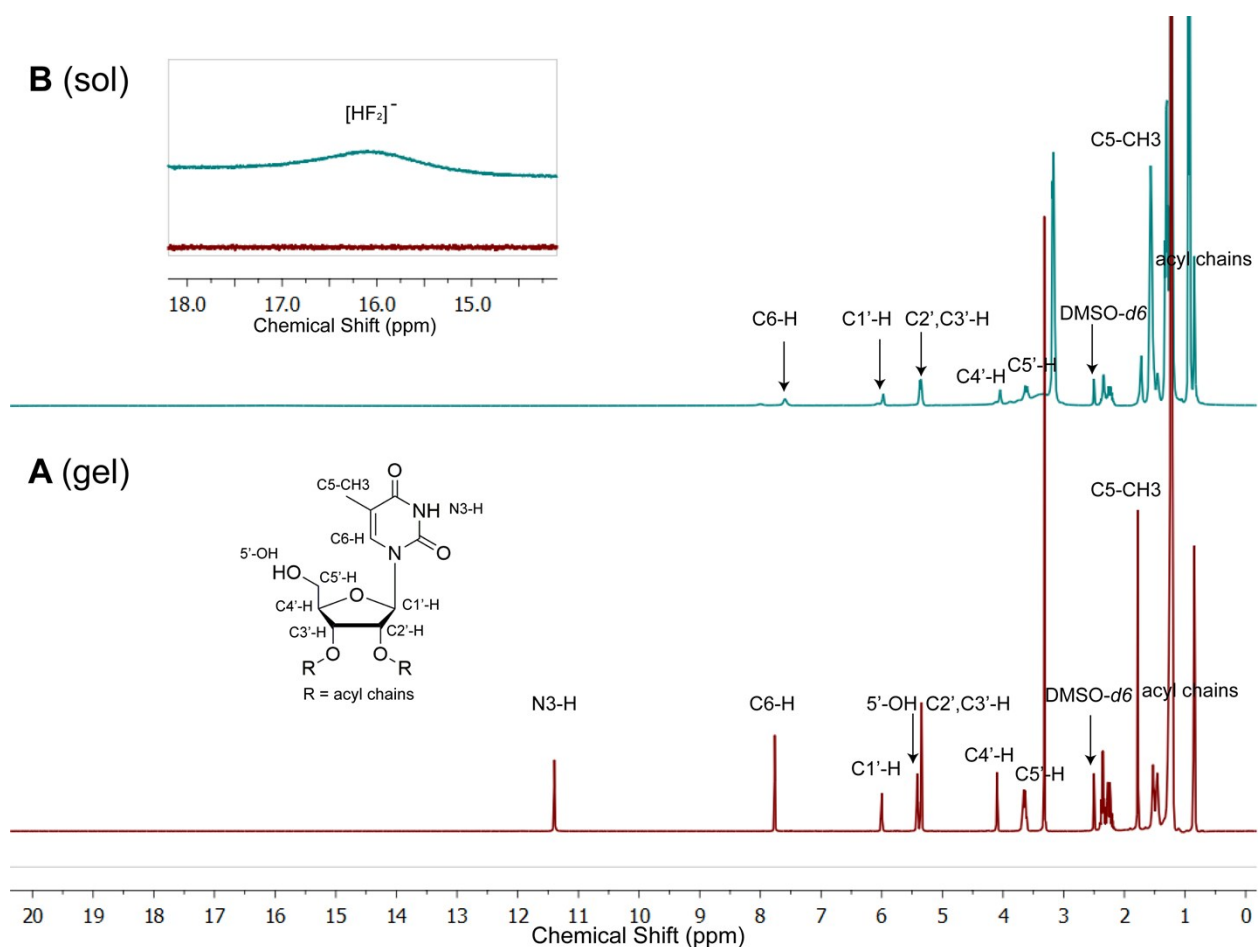


Fig. S9 ¹H NMR spectrum of nucleolipid **7b** in *d*₆-DMSO (3.2 w/v %) in the absence (**A**, gel state) and presence of 1 equiv. of fluoride ion (**B**, sol state). The disappearance of N3-H, 5'-OH signals and appearance of a new triplet signal at 16.05 ppm corresponding to HF₂⁻ confirms the deprotonation of imino hydrogen atoms by fluoride anion. Similarly the C6-H signal shifted towards up field C6-H when the fluoride ion deprotonate N3-H.

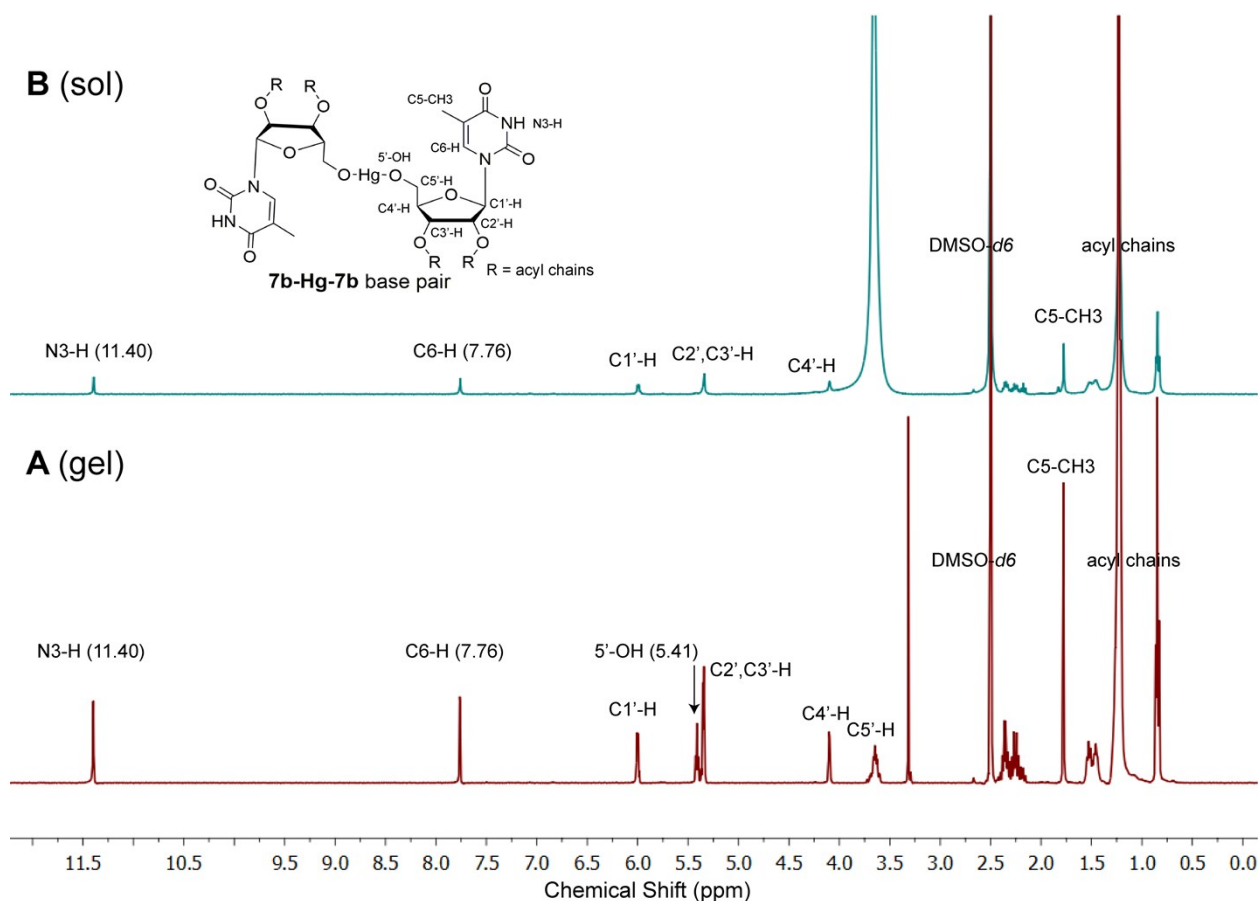


Fig. S10 ^1H NMR spectrum of nucleolipid **7b** in d_6 -DMSO (3.2 w/v %) in the absence (**A**, gel state) and in the presence of 1 equiv. of Hg^{2+} ion (**B**, sol state). The disappearance of 5'-OH (5.41 ppm) signal but N3-H (11.40 ppm) intact in both phases. The mode of binding of Hg^{2+} is 5'-O-Hg-O-5' with respective sugar moiety of nucleolipid **7b**.

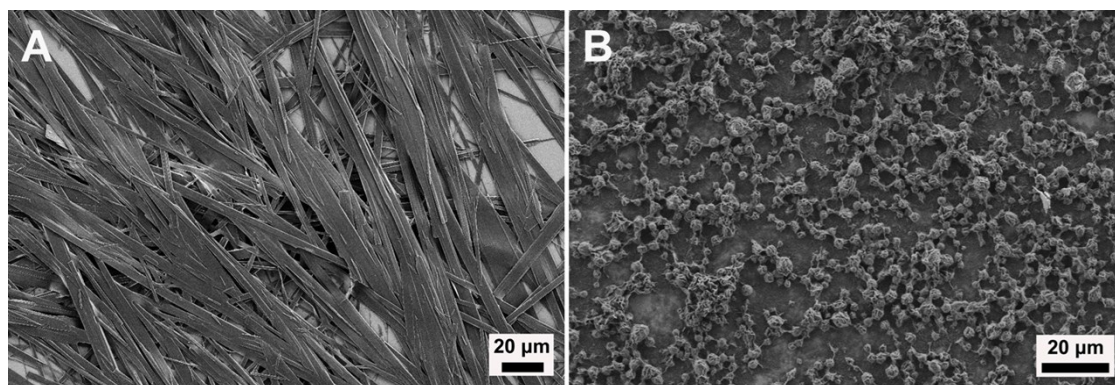


Fig. S11 FESEM images of nucleolipid **7d** gel (**A**) in the absence and (**B**) in the presence of Hg^{2+} ions.

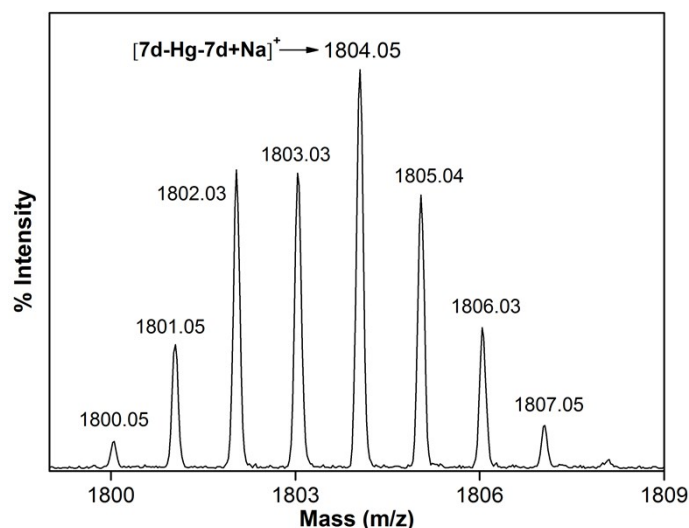


Fig. S12 Mass spectrum showing the molecular ion peak of the 7d-Hg-7d base pair complex (**7d-Hg-7d+Na⁺**) calculated mass 1803.90, found mass 1804.05. Characteristic isotopic pattern supports the presence of Hg²⁺ ion.

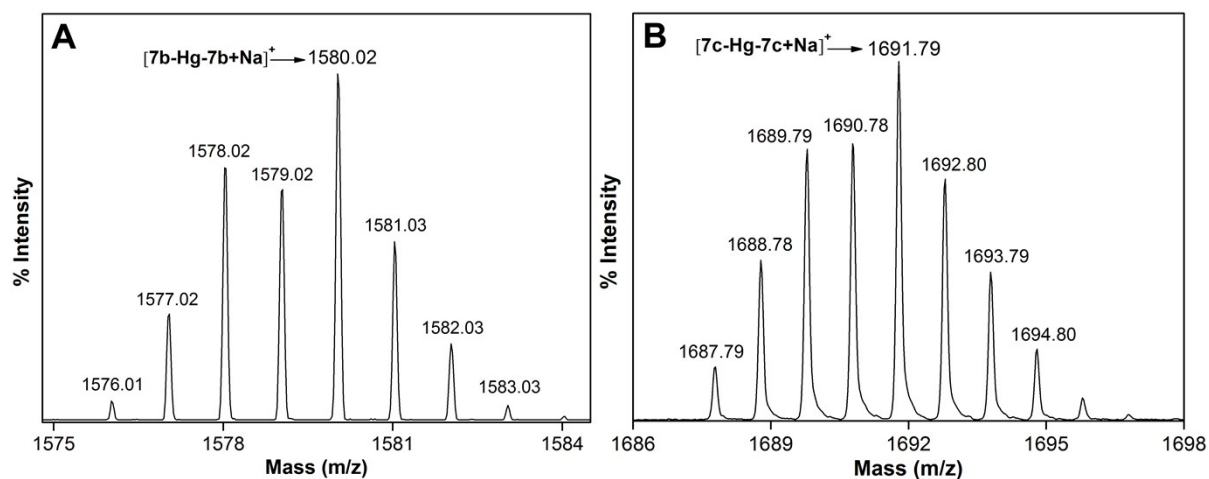
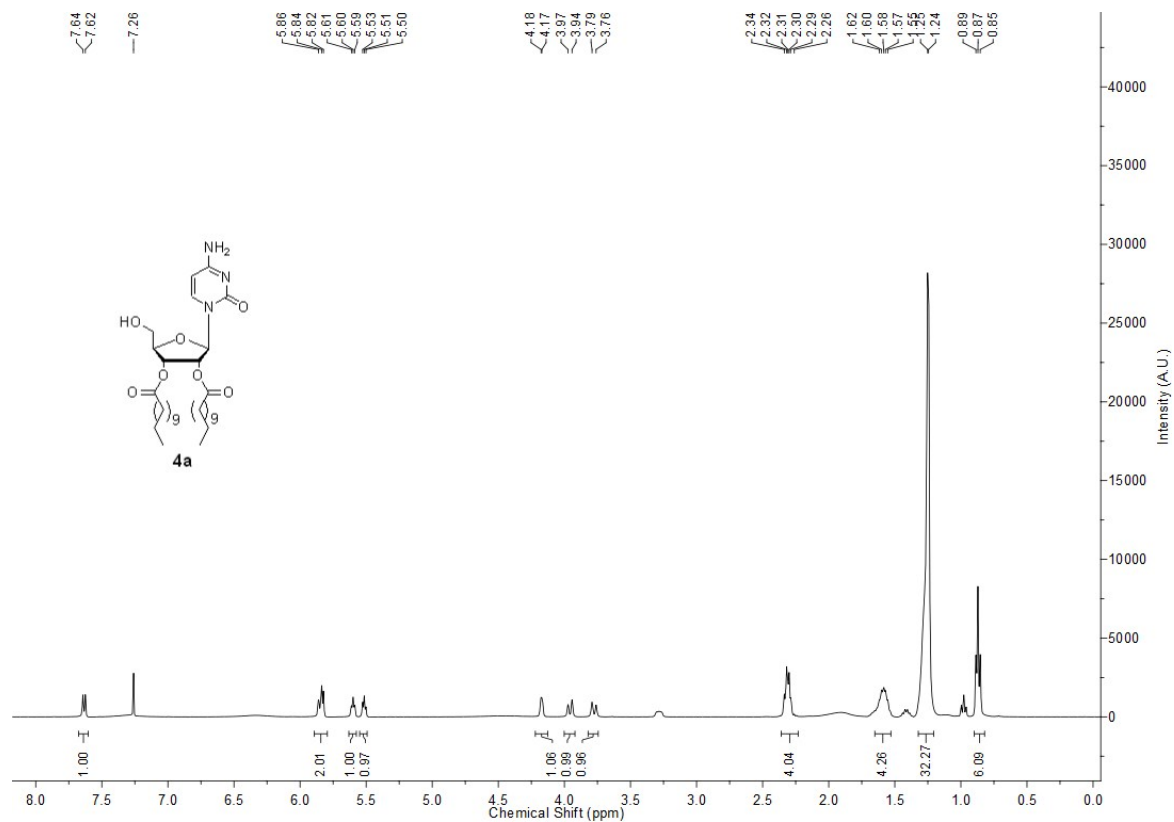


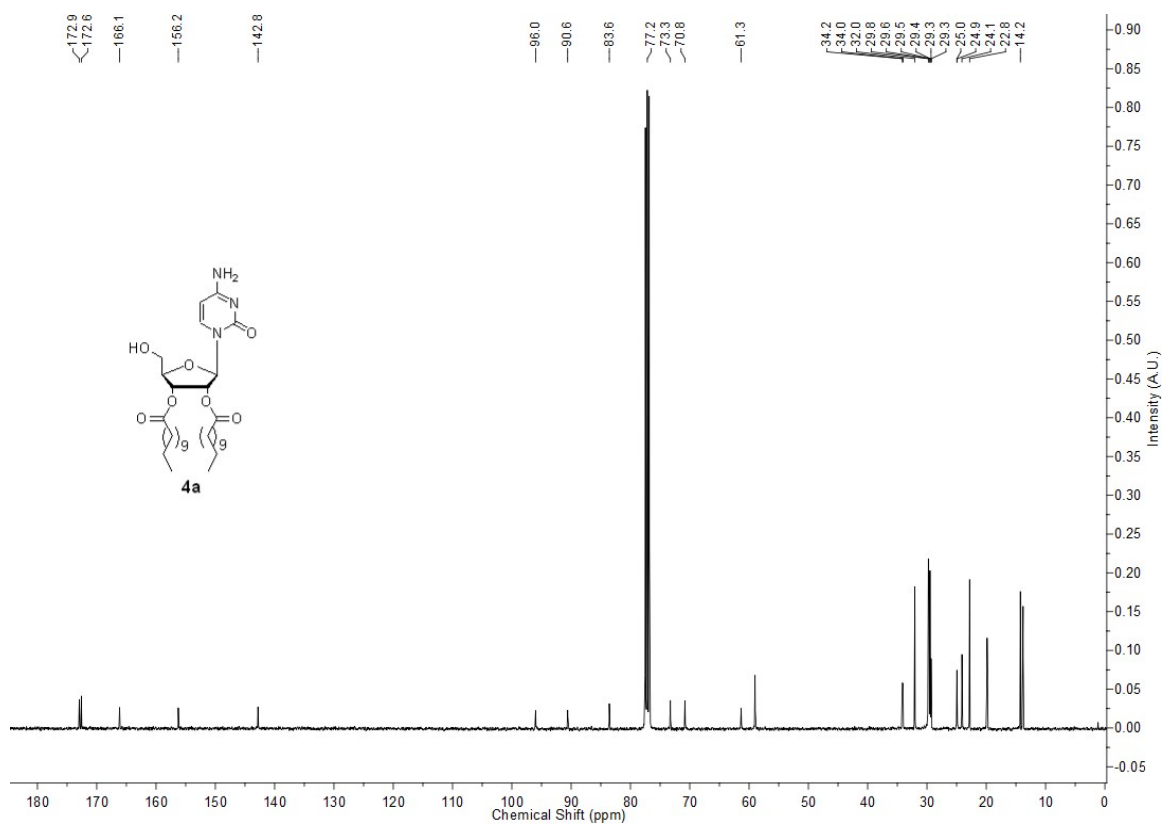
Fig. S13 (A) Mass spectrum showing the molecular ion peak of the 7b-Hg-7b base pair complex (**7b-Hg-7b+Na⁺**) calculated mass 1579.47, found mass 1580.02. (B) Mass spectrum showing the molecular ion peak of the 7c-Hg-7c base pair complex (**7c-Hg-7c+Na⁺**) calculated mass 1691.68, found mass 1691.79. Characteristic isotopic pattern supports the presence of a Hg²⁺ ion.

6. NMR spectra

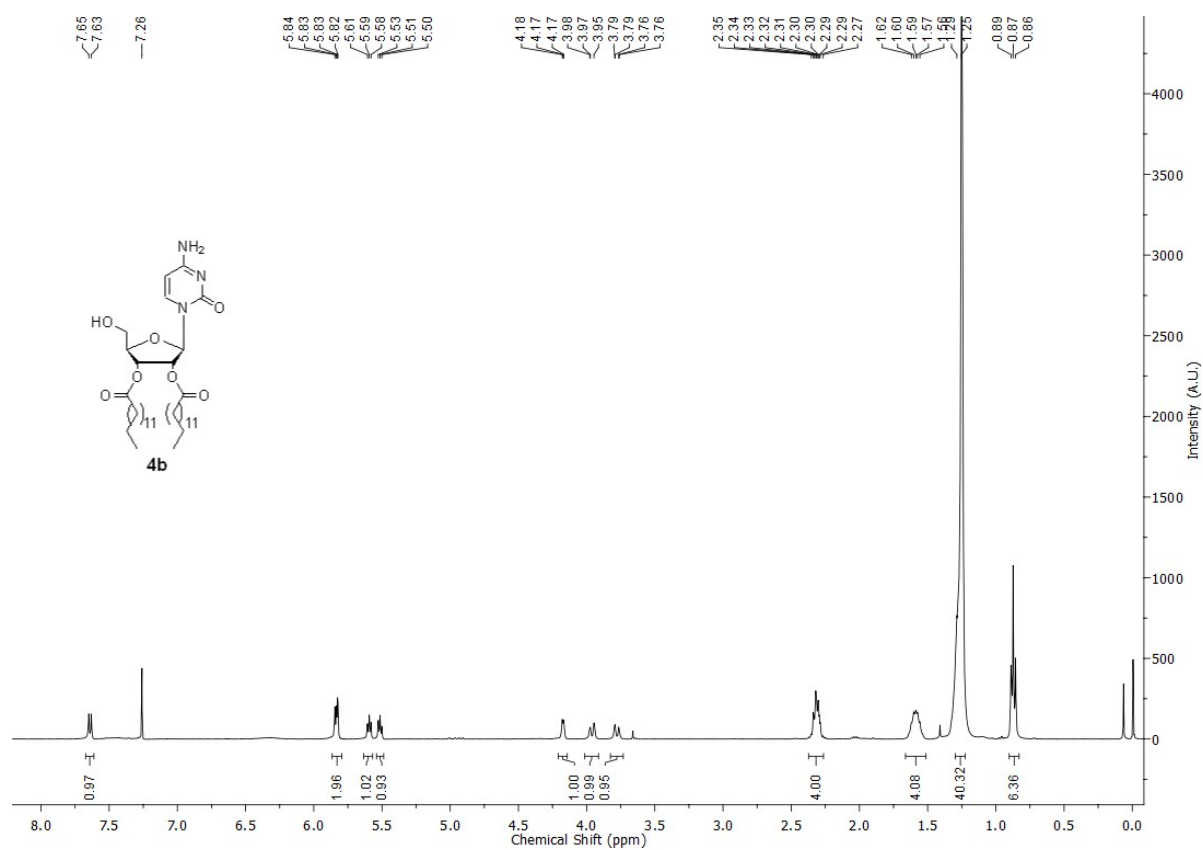
^1H NMR of nucleolipid **4a** in CDCl_3



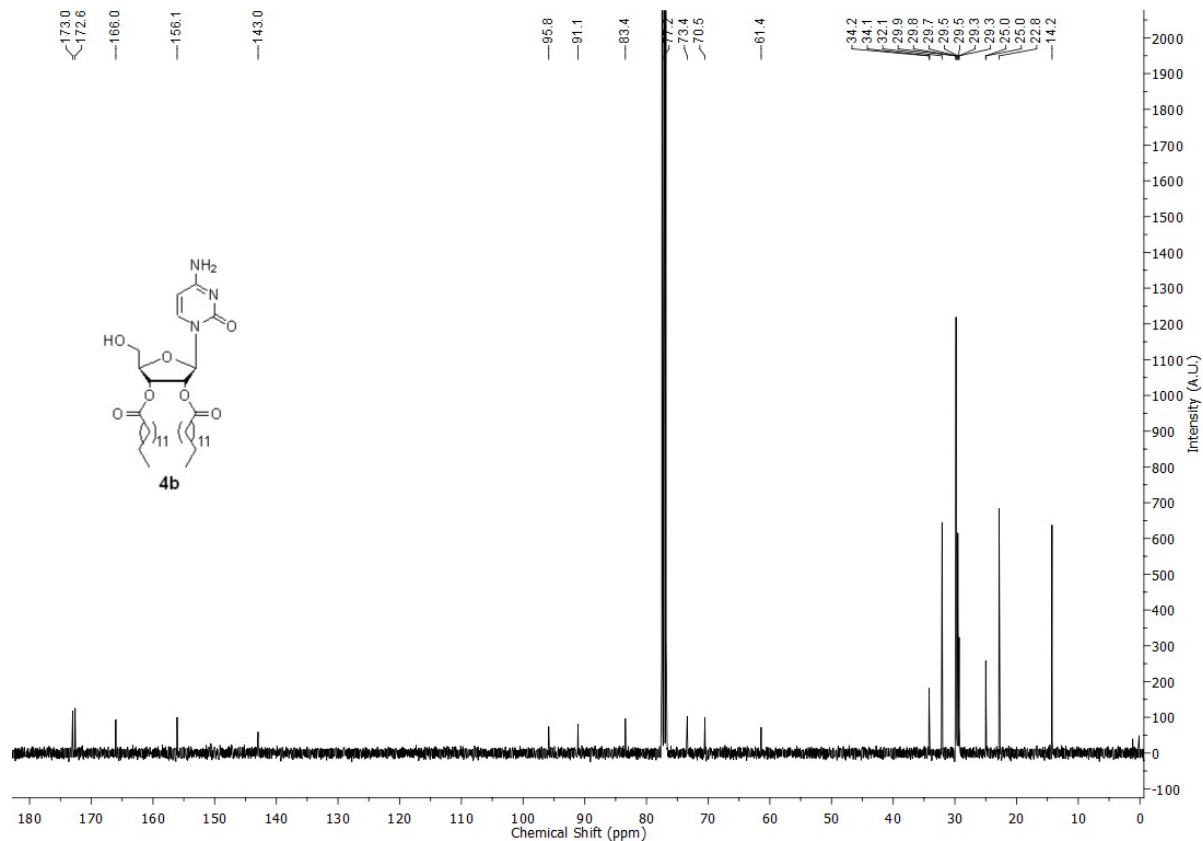
^{13}C NMR of nucleolipid **4a** in CDCl_3



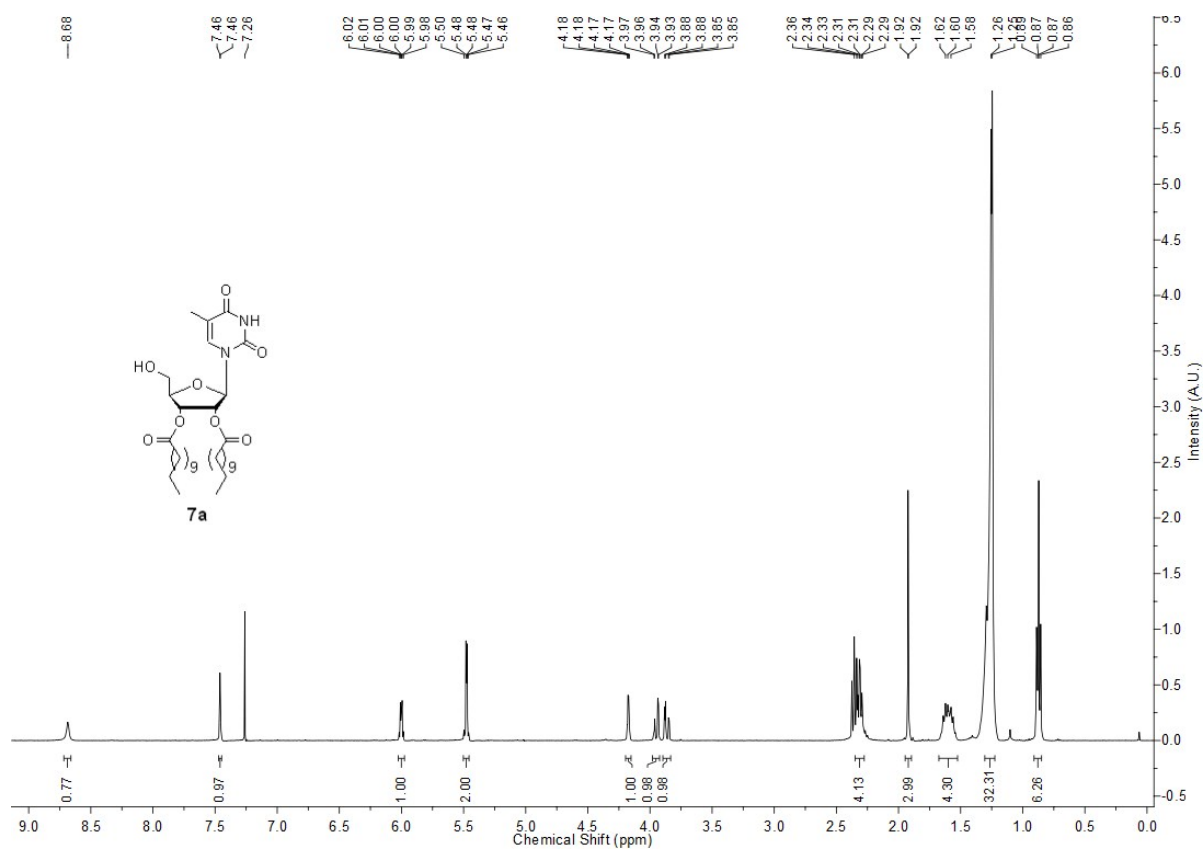
^1H NMR of nucleolipid **4b** in CDCl_3



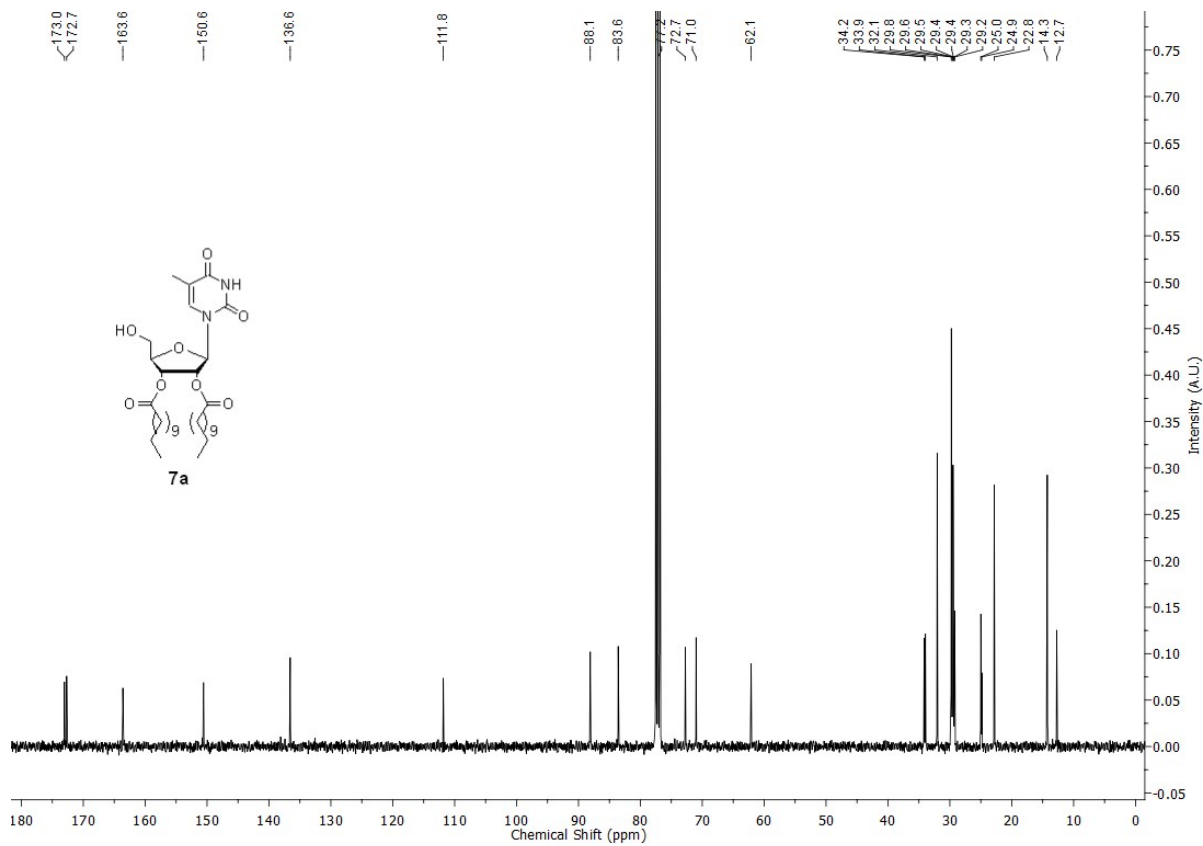
^{13}C NMR of nucleolipid **4b** in CDCl_3



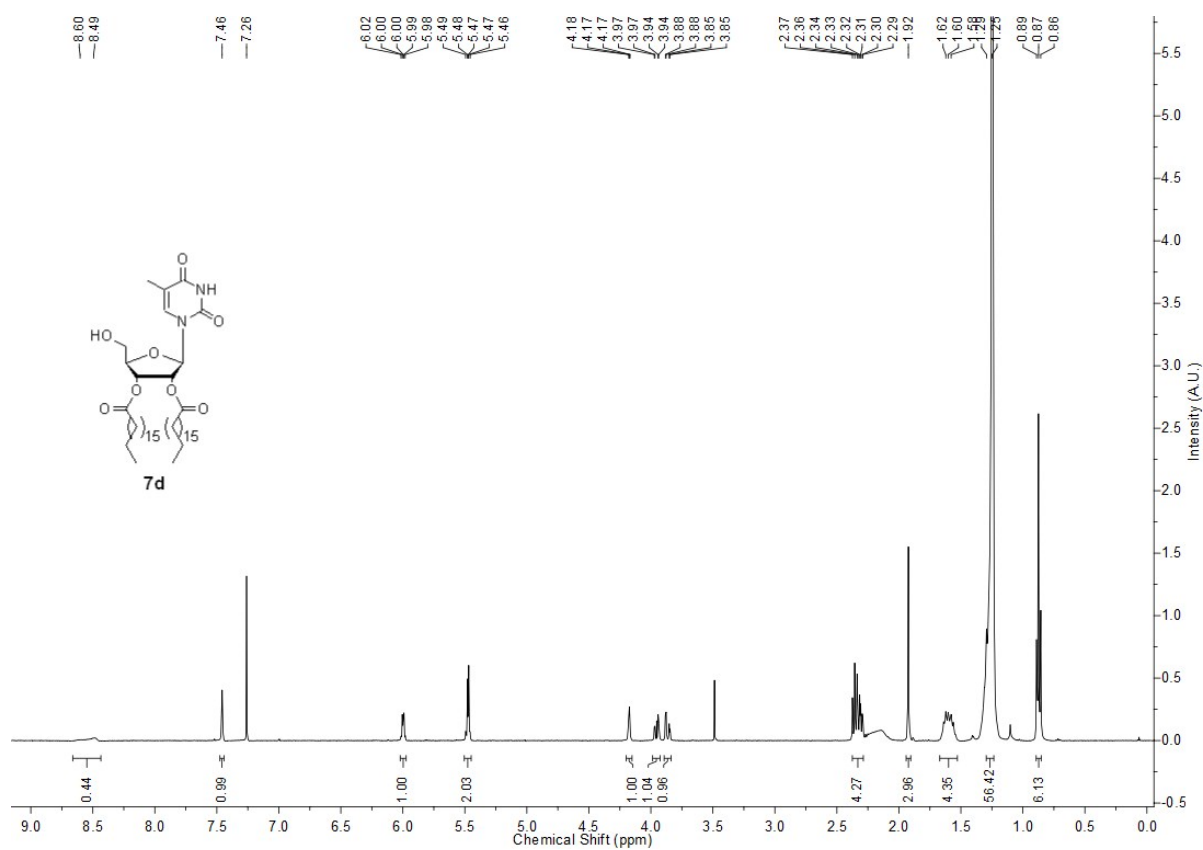
^1H NMR of nucleolipid **7a** in CDCl_3



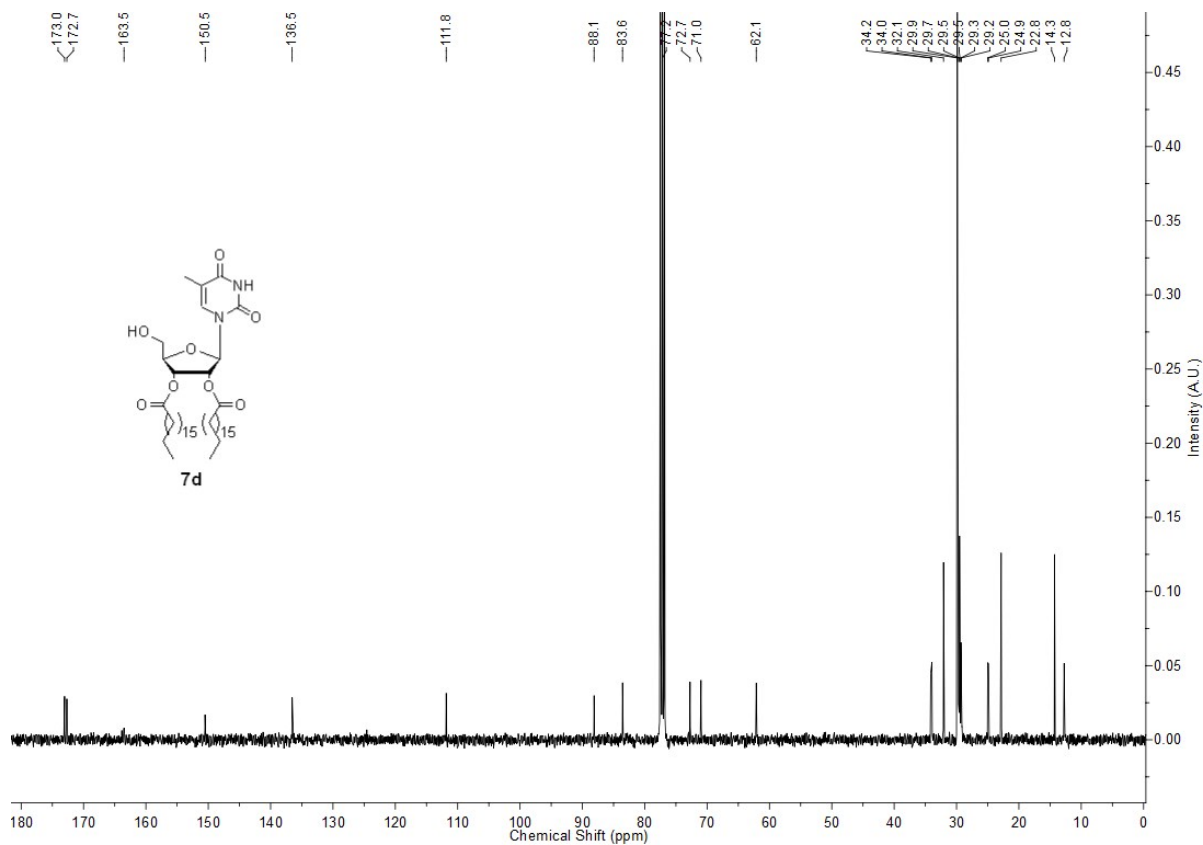
^{13}C NMR of nucleolipid **7a** in CDCl_3



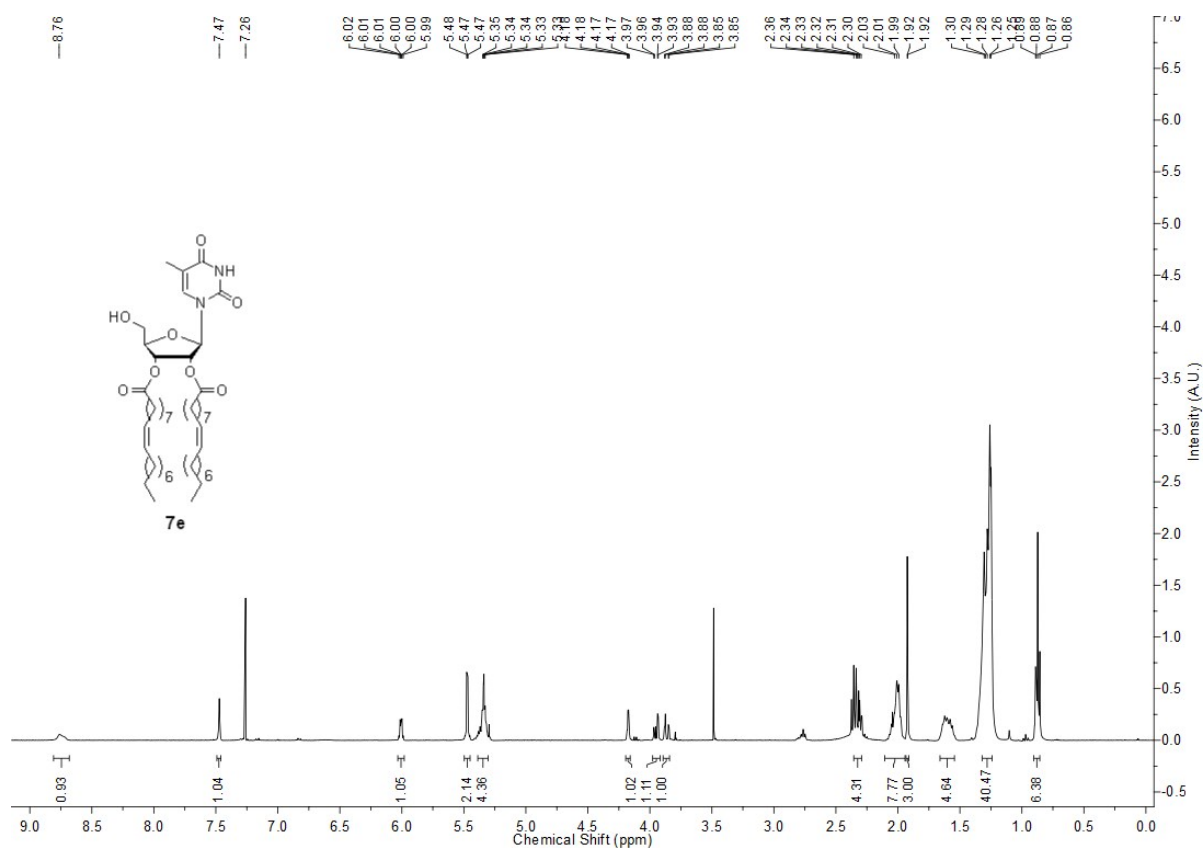
¹H NMR of nucleolipid **7d** in CDCl₃



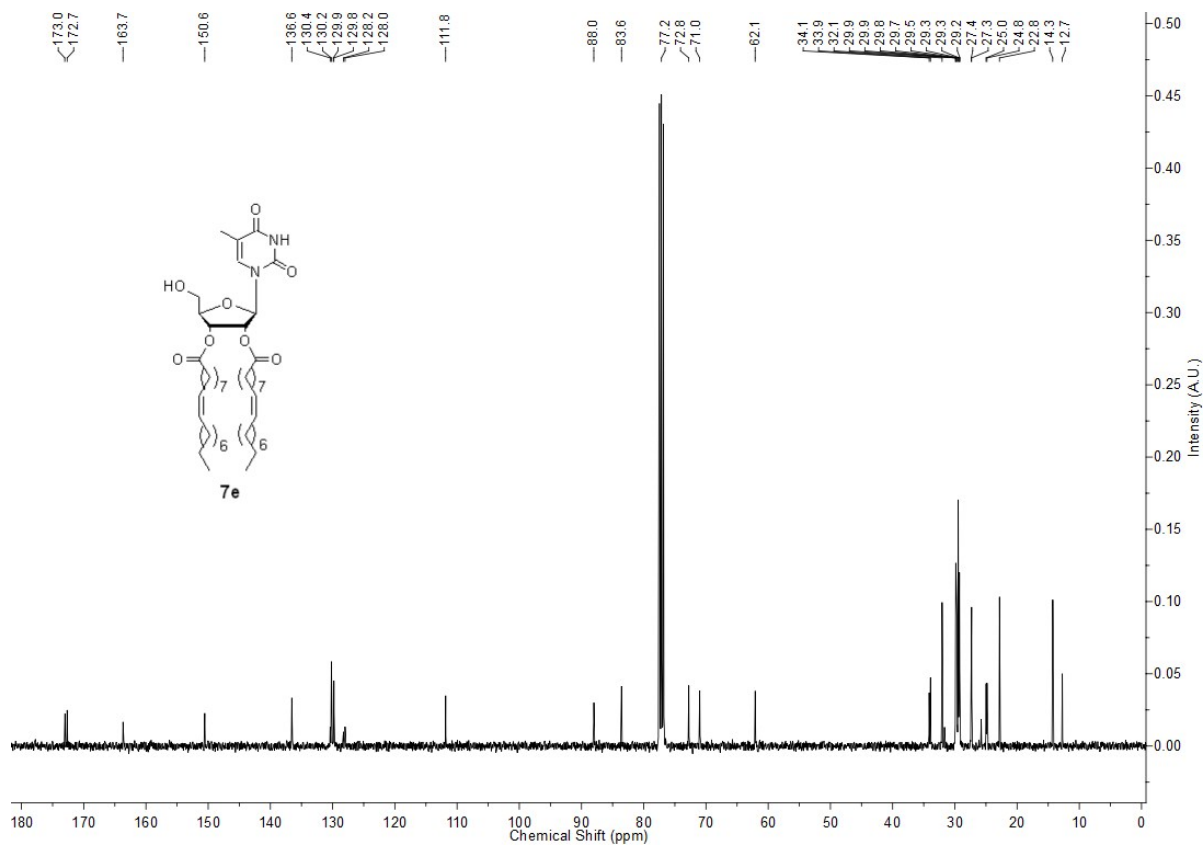
¹³C NMR of nucleolipid **7d** in CDCl₃



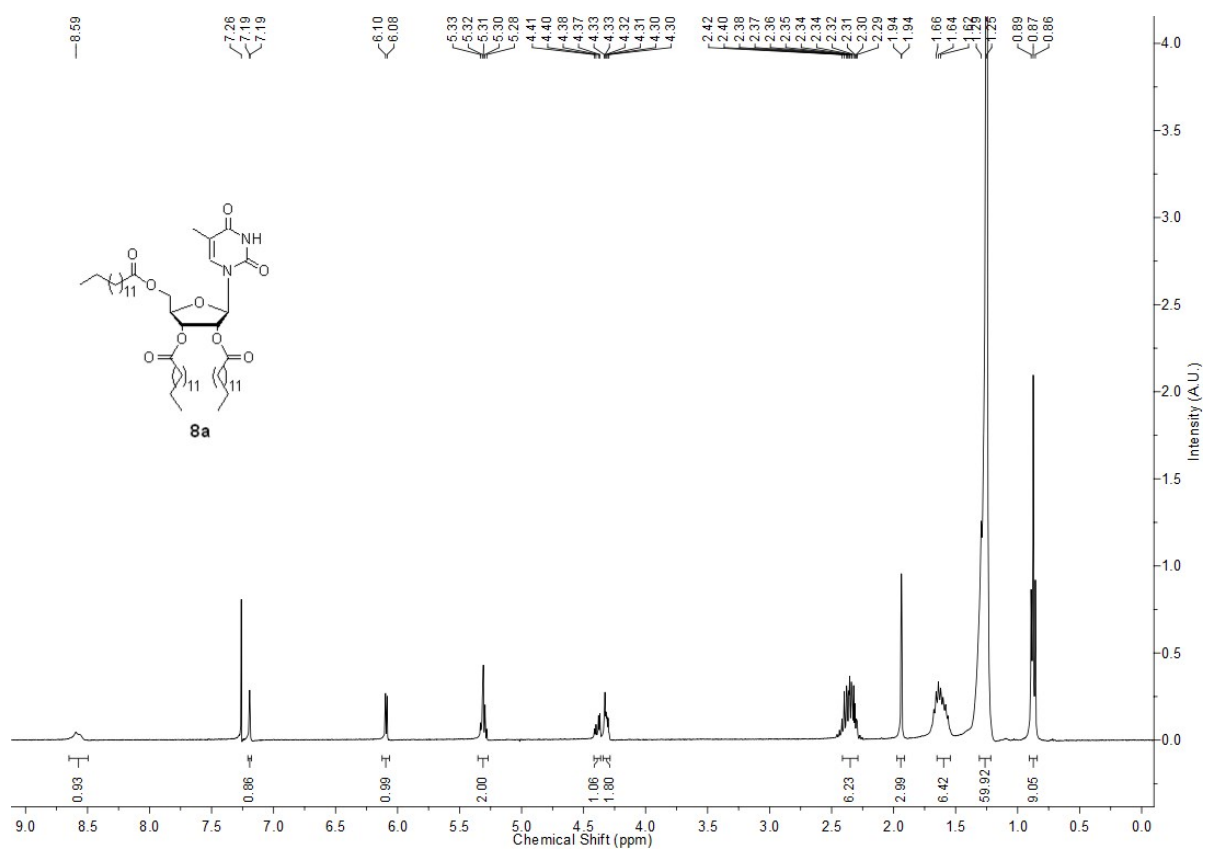
¹H NMR of nucleolipid **7e** in CDCl₃



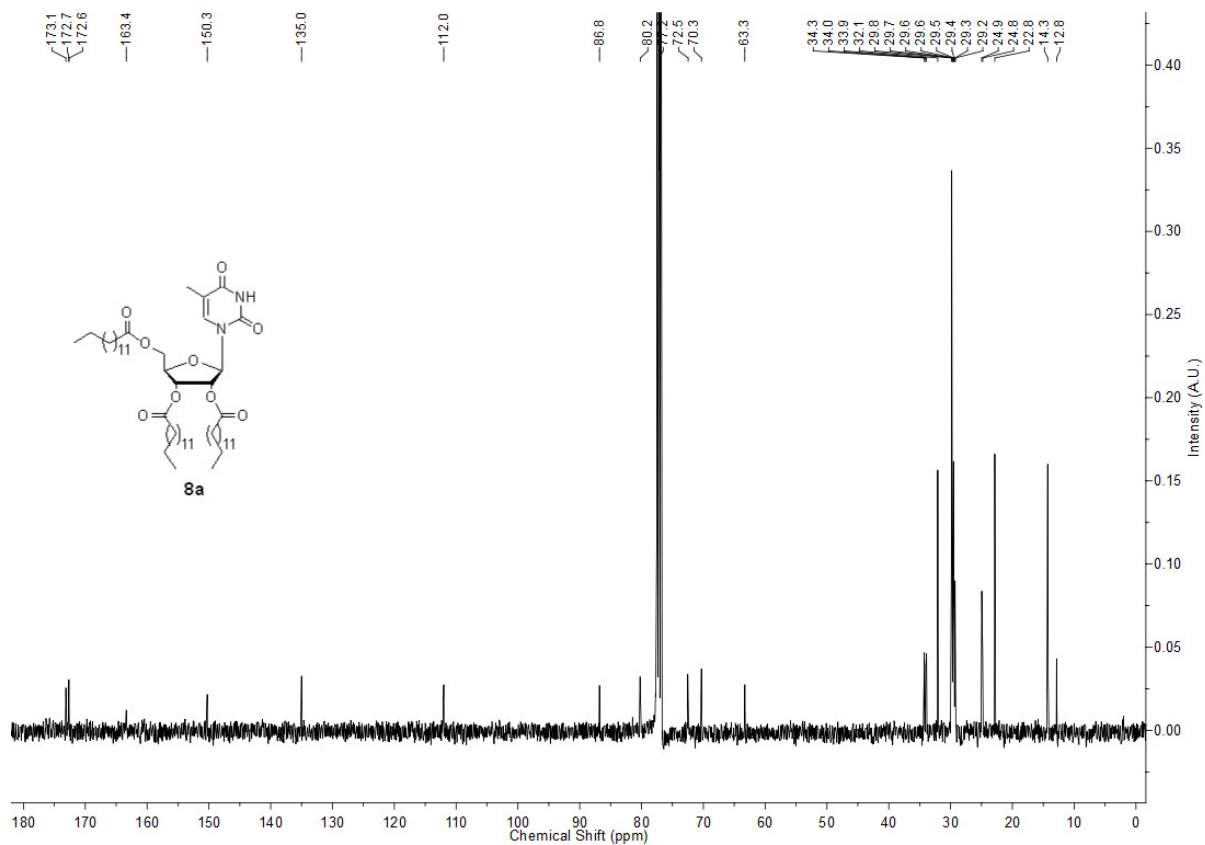
¹³C NMR of nucleolipid **7e** in CDCl₃



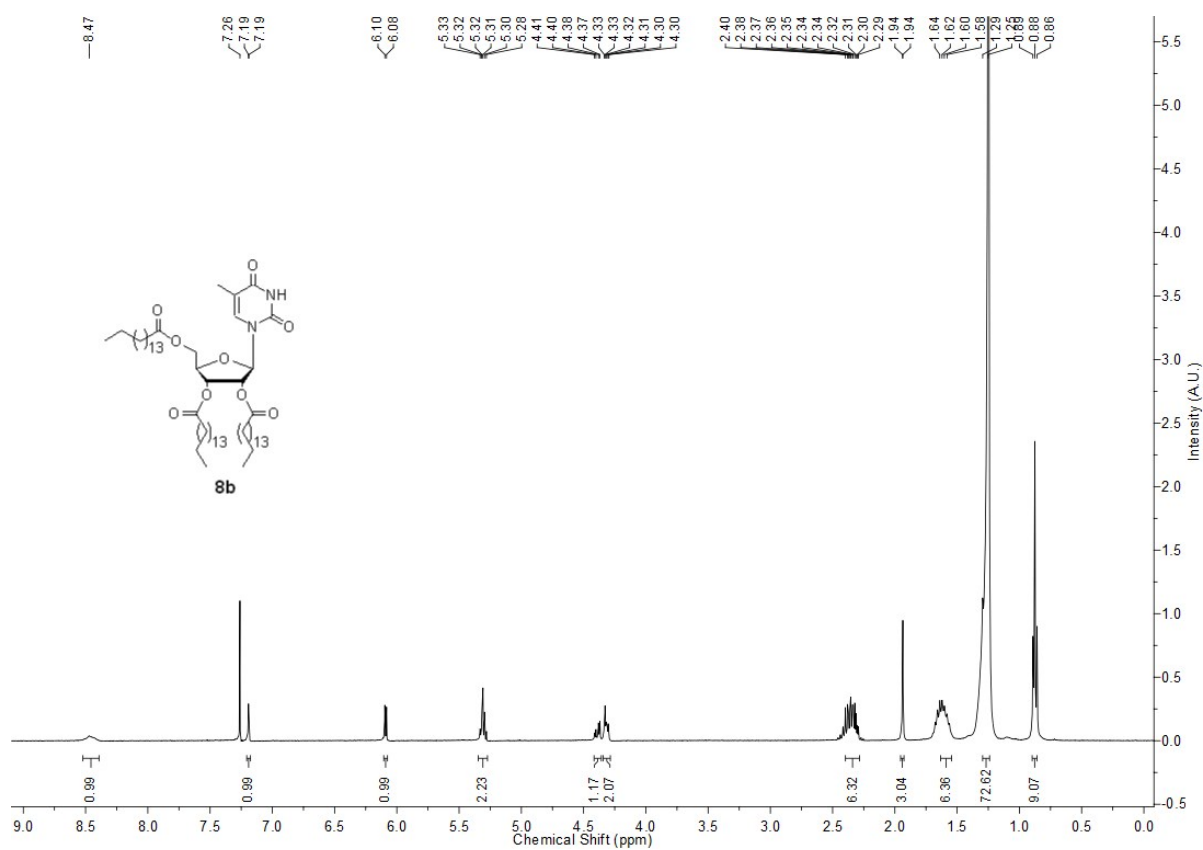
^1H NMR of nucleolipid **8a** in CDCl_3



^{13}C NMR of nucleolipid **8a** in CDCl_3



¹H NMR of nucleolipid **8b** in CDCl₃



¹³C NMR of nucleolipid **8b** in CDCl₃

